universität wien

MASTERARBEIT

Titel der Masterarbeit

Mechanisms of zoledronate – induced γδ T-cell activation

Verfasserin

Juliana Komuczki, BSc

angestrebter akademischer Grad

Master of Science (MSc)

Wien, 2013

Studienkennzahl lt. Studienblatt:	A 066834
Studienrichtung lt. Studienblatt:	Masterstudium Molekulare Biologie
Betreuerin:	Univ.-Prof. Dr. Manuela Baccarini

This master thesis was performed at the

Medical University Innsbruck

Department of Urology &

K1 Centrum Oncotyrol, Center for Personalized Cancer Therapy

Laboratory for Immunology and Immunotherapy

Innrain 66a
6020 Innsbruck, Austria

and was supervised by

Ao. Univ.-Prof. Dr. Martin Thurnher

“Discovery is to see what everyone else has seen and to think what no one else has thought”

Albert von Szent-Györgyi Nagyrapolt
1937 Nobel Laureate in Medicine

FOREWORD AND ACKNOWLEDGEMENTS

Foreword

With my master thesis work in the Laboratory for Immunology and Immunotherapy of the Department of Urology, headed by Univ.-Prof. Martin Thurnher, I have contributed as a coauthor to a manuscript, which was published in the Journal of Immunology (DOI number: 10.4049/jimmunol.1300603,). With permission of the American Association of Immunologists (AAI) figures from this article were also used for the present master thesis.

Essential Requirements of Zoledronate-Induced Cytokine and γδ T Cell Proliferative Responses
Oliver Nussbaumer, Georg Gruenbacher, Hubert Gander, Juliana Komuczki, Andrea Rahm, and Martin Thurnher, J Immunol 1300603; published ahead of print June 21, 2013, doi:10.4049/jimmunol.1300603

Acknowledgements

I want to express my thanks to the following people who have enabled my master thesis and have supported my work.

Especially I want to give my sincerest gratitude to my supervisor, Univ.-Prof. Martin Thurnher, head of the Laboratory for Immunology and Immunotherapy, not only for giving me the chance to be part of his research team, but also for supporting and supervising me throughout my thesis with his constant patience, invaluable assistance and knowledge as well as for accurate proofreading my thesis.

I would also like to thank Univ.-Prof. Baccarini for her agreement of being my official supervisor of this thesis.

In my daily work routine I have been blessed to work with a friendly working group. For the great working atmosphere and the excellent teamwork I would like to gratefully acknowledge all my colleagues. I want to thank Hubert Gander for helpful teaching and supervising my experiments as well as always being available for questions. I thank Georg Grünbacher, PhD and Oliver Nussbaumer, PhD for their useful advices for planning and performing experiments, for always being supportive and available for consultation as well as for proofreading my thesis. In the future I also wish to be a similar co-worker of the same value as you two have been to me and during my work I have learnt a lot from you. I also want to thank Mag. Andrea Rahm for teaching, her support in CBA flex set measurements. I also want to thank Bernhard Steiner, BSc, who was not only a perfect working partner but also for proofreading one of the earlier drafts as well as for his love and support.

Furthermore I would like to thank Barbara Frick, PhD (Research Manager of Oncotyrol- K1 Centrum, Center for Personalized Cancer Therapy) for helping to successfully apply for a FEMtech grant of the BMVIT – Federal Ministry for Transport, Innovation and Technology, which funded my master thesis.

I also would like to express my deepest thanks to my parents Maria and Andreas Komuczki for providing me not only the opportunity of a good education but also for their constant support and believe in my academic career.
To my older brother Johannes Komuczki, who inspired me during my studies and who will never lose his courage and take his fate into his own hands. Life is for living!
To my twin sister Christina Komuczki, for being my best friend and always being supportive.

Last but not least I want to thank my good friend Magdalena Schwarz, Bsc for her support during my master's study and especially for proofreading my master thesis.

CONTENTS

1. Aims of the study

Zoledronate is currently the most potent and widely prescribed nitrogen-containing bisphosphonate (N-BP), which can directly influence tumour biology and may show indirect antitumour effects. N-BPs inhibit farnesyl pyrophosphate (FPP) synthase, a key enzyme in the mevalonate pathway. The mevalonate pathway provides isoprenoid building blocks, which include cholesterol and protein prenylation. Already decades ago it was demonstrated that upstream accumulation of isopentenyl pyrophosphate (IPP) due to zoledronate-mediated FPP interference specifically activates γδ T cells. However, consequences of zoledronate interference with the mevalonate pathway and the resulting depletion of the downstream intermediates have been investigated and understood poorly so far. In the present master thesis I have focused on early upregulation of surface markers and cytokine production as well as γδ T-cell expansion.

Specific Aims:

- How does downstream depletion of the prenyl pyrophosphates influence the cytokine response?
- How does downstream depletion of the prenyl pyrophosphate affect γδ T-cell proliferative response?
- What would be the effect of supplementation with prenyl pyrophosphates?
- How can γδ T-cell expansion be improved?

2. Introduction

2.1 Mevalonate metabolism

The mevalonate pathway, which is present in all higher eukaryotes and many bacteria, provides isoprenoid building blocks, which include cholesterol, constituent of membrane structures; dolichol, required for N-glycosylation; and the farnesyl- and geranyl groups necessary in the protein prenylation step (1). First in the mevalonate pathway, the hydroxymethyl-glutaryl coenzyme A (HMG-CoA) reductase converts HMG-CoA to mevalonate, which is further converted to IPP and dimethylallyl pyrophosphate (DMAPP). The FPP synthase converted FPP by DMAPP and two units of IPP. Further gernalygeranyl pyrophosphate (GGPP) is generated from FPP by the GGPP synthase **(Fig. 3)**. FPP is the isoprenoid precursor of cholesterol and other sterols (2). Moreover the two intermediates GGPP and FPP serve as substrates for prenylation, a posttranslational modification. Thereby the protein prenyltransferase catalyses the attachment to these prenyl groups on different proteins in the cell, mainly on small GTPases such as Ras, Rho and Rac (3). Imbalances within this pathway can result in diseases such as cancer and cardiovascular disease. A previous study provided evidence that the mutant form of p53 can significantly upregulate the mevalonate pathway-activity, which can contribute to malignancy. These observations confirm the fact that the mevalonate pathway is an important therapeutic target (4), (5).

2.2 Nitrogen-containing bisphosphonates (N-BPs)

There are two groups of bisphosphonates; the non-nitrogen bisphosphonates, like etidronate and clodronate and the more potent N-BPs, such as pamidronate, risedronate, ibandronate, alendronate and zoledronate [**Fig. 1**, (6)]. FPP synthase can be inhibited by N-BPs, also referred to as aminobisphosphonates, resulting in the accumulation of IPP that can be generated into a novel ATP analogue 1-adenosin-5′-yl ester 3-(3-methylbut-3-enyl) ester (ApppI) and leads to depletion of FPP and GGPP (7), (8).

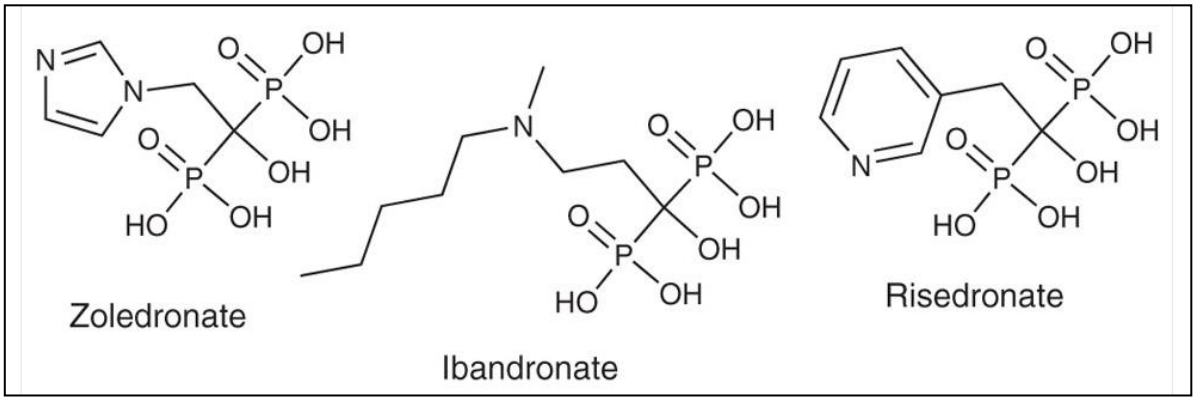

Figure 1: Chemical structure of the most potent N-BPs in clinical use: *zoledronate, ibandronate and risedronate. [figure adapted from (9)]*

The loss of FPP and GGPP can prevent protein prenylation and thus attachments of signaling proteins to the cell membrane leading to defects in signaling pathways and to apoptosis (10). Osteoporosis and other similar bone diseases are major applications of N-BPs since osteoclasts take up N-BPs, which leads to cell death. This effect is also exhibited in tumour cells (11), (12). Therefore the anticancer effect of N-BPs is also established for treatment of metastatic bone disease of multiple myeloma (13), breast (14) and prostate cancer (15).

During bone resorption the osteoclasts take up N-BPs concentrated in the mineral bone which leads to cell death. The apoptotic effect is caused by the inhibition of protein prenylation and the accumulation of the pro-apoptotic ATP analogue ApppI (12).

The N-BPs interfere with the mevalonate pathway (**Fig. 3)** as they are analogues of prenyl pyrophosphates, which are highly resistant to enzymatic hydrolysis due to the P-C-P backbone instead of P-O-P structure [(10), (**Fig. 2**)]**.**

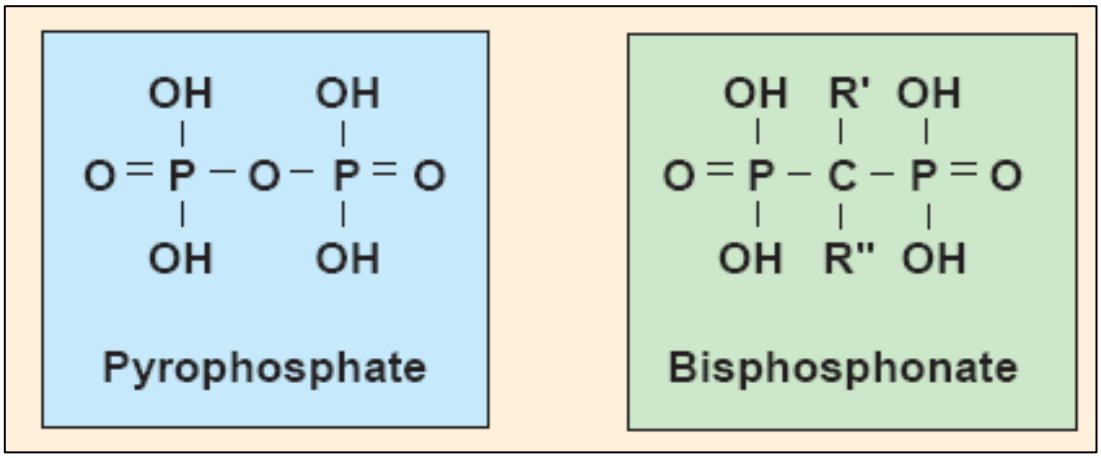

Figure 2: The structure of pyrophosphates compared to the structure of bisphosphonates: *The bisphosphonate structure with the central carbon is more stable compared to the structure of the pyrophosphate with the central oxygen atom (10). [figure from (16)]*

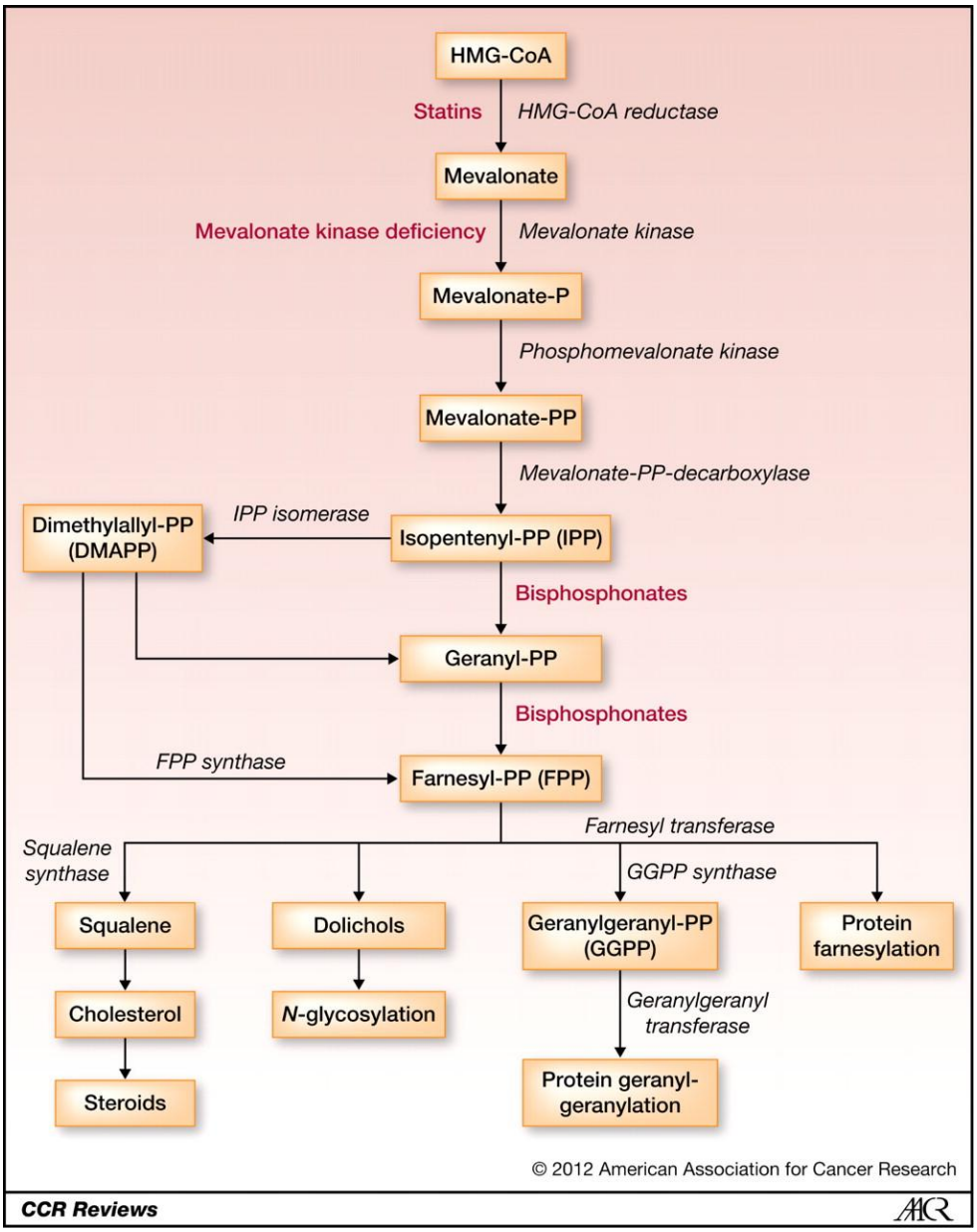

Figure 3: Scheme of the mevalonate pathway: *First in the mevalonate pathway the HMG-CoA reductase converts HMG-CoA to mevalonate, which can be inhibited by statins. Mevalonate can be further metabolized to IPP and DMAPP. The FPP synthase can be inhibited by N-BPs, resulting in accumulation of IPP that can be converted to ApplI and leads to depletion of FPP and GGPP (7). The mevalonate kinase deficiency is a rare inborn metabolism error leading to an autoinflammatory syndrome (17).*

Through the inhibition of the FPP synthase γδ T cells can be activated by the accumulation of IPP and its stereoisomer DMAPP (12), (18). [Figure from (2)]

2.3 T cell receptor and γδ T cells

T cells, alongside with B cells, represent the second effector cell type of the adaptive immune system. These cells can be divided into two groups: the αβ T cells, belonging to the adaptive immune system and the γδ T cells, which have innate-like functions as they rapidly secrete cytokines and also exhibit cytotoxic effects. Both αβ T cells and γδ T cells express a CD3-associated T-cell receptor [TCR, (19), (20), (21)].

In the human body 3 to 5 % of the lymphocytes are γδ T cells, which generate the γδ TCR using a variety of different V(D)J recombinations via the recombination activating gene (RAG). Most of these cells, which typically develop in the thymus, have a Vγ9Vδ2 TCR [>70 %, (22), (23)]. The γδ T cells are rarely localized in the spleen, lymph node parenchyma, Peyer's plaques and thymus. However they are abundantly found in the intestine as intraepithelial lymphocytes (IELs). In the skin of mice they are commonly found as dendritic epidermal T cells [DETC, (24), (25)]. γδ T cells can sample various non-peptide-antigens and expand clonally. Through their readily activation, large numbers of γδ T cells can rapidly be provided for defense against pathogens and tumour cells by clonal expansion. Furthermore the monoclonal or oligoclonal use of the TCR is an important crossover of adaptive and innate immune functions (23).

γδ T cells have cytolytic functions and produce a variety of cytokines, which promote activation of macrophages, neutrophils and lymphocytes. In addition, γδ T cells have structural as well as antigen-binding characteristics. They acquire antigen feature properties and therefore can present antigens and enable adaptive immune response as well as they are able to regulate inflammation (26), (27).

Surface markers of γδ T cells

Whereas peripheral αβ T cells usually express either CD4 or CD8 on their surface, which are elements of major histocompatibility complex (MHC) peptide presentation, most of the peripheral γδ T cells are double negative for CD4 and CD8 (28), (24). This consists with the fact that γδ T cells do not recognise MHC associated peptides (18). Vγ9Vδ2 T cells in adults exhibit a pre-activated ("memory") phenotype as they express a CD45RO surface marker, whereas most of the Vγ9Vδ2 T cells in the cord blood lack CD45RO.

Similar to αβ T cells, Vγ9Vδ2 T cells are divided into four different groups based on their surface markers CD45RA and CD27, which belong to the TNF receptor family and have costimulatory effects (19), (29):

a.) naïve T cells (T_{naive}), which express both CD45RA and CD27,
b.) central memory T cells (T_{CM}), which lack CD45RA but are still CD27 positive
c.) effector-memory T cells (T_{EM}), which are double negative for CD45RA and CD27
d.) terminally differentiated T cells (T_{EMRA}), which re-express CD45RA but lack CD27.

Antigen recognition

As γδ T cells control the barrier surfaces in an innate-like manner, they have to react immediately against pathogens and initiate an inflammatory response (30).
While αβ T cells recognise peptide antigens bound to MHC it is still unknown how γδ T cells are stimulated by these small non-peptide antigens such as foreign IPP or bacterial products such as (E)-4-hydroxy-3-methyl-but-2-enyl pyrophosphate [HMB-PP, (18)]. Nevertheless, γδ T cells recognise antigens without the requirement of antigen presenting cells (APCs), e.g. dendritic cells (DCs) and these antigens do not have to be presented by MHC molecules (27).

2.4 The immune stimulatory effect of N-BPs on γδ T cells

N-BPs exhibit immune stimulatory effects, which were first identified as a side effect during the treatment of bone diseases resulting in a higher percentage of γδ T cells in peripheral blood (31). γδ T cells can be activated early by viral glycoproteins generated from herpes viruses, and by phosphoantigens, the intermediates either from the non-mevalonate pathway generating HMB-PP, which are produced by a variety of microorganisms (32) or from the mevalonate pathway. In the mevalonate pathway through the inhibition of the FPP synthase, γδ T cells can be activated by the accumulation of IPP and its stereoisomer DMAPP, both ligands of the Vγ9Vδ2 T cells (12), (18). As IPP is an intermediate of the mevalonate pathway of higher eukaryotes and many bacteria, the human Vγ9Vδ2 T cells have a cross-reactivity between foreign and self phosphoantigens (23).

The stimulation of Vγ9Vδ2 T cells against tumour cells can be improved in combination with synthetic phosphoantigens, tumour cells or APCs like monocytes and DCs (12). Moreover, it has been reported that the activation of Vγ9Vδ2 T cells is improved by interactions between Vγ9Vδ2 T cells and monocytes through soluble factors, contact-dependent interactions and monocyte survival as well as differentiation into DCs (33).

Despite this, it is still not known whether γδ TCR recognises antigens independently or if phosphoantigens are presented in the context of an unknown surface molecule. The adaptive TCR specificities of γδ TCR through the variety length of the γδ TCR complementarity-determining region 3 (CDR3) loops is conferred by the architecture of the TCRD locus. It has been claimed that through the diversity in length of the CDR3 loops, the γδ TCR recognises antigens, which do not necessarily have to be presented by some specific presenting element (23).

It might be possible that the γδ TCR binds antigens using conserved parts in their CDR3 and therefore are only activated by a few numbers of antigens (34).

2.5 Tumour biology and immuntherapy using γδ T cells

It has been observed that IPP is accumulated in malignant cells and γδ T cells recognise these cells quickly with their TCR. Additionally, these lymphocytes can also react to the natural killer group 2, member D (NKG2D) ligands such as F1-ATPase, to stress molecules like MHC class I chain-related molecules A and B (MICA and MICB), to UL16-binding protein (ULBP) 1 - 4 as well as to retinoic acid early transcript 1. These molecules appear on the surface of infected, stressed or malignant cells (35).

Immunotherapy using γδ T cells is promising as cancer therapy because of their high potential to produce interferon-γ (IFN-γ), pronounced cytoxicity and their MHC independent recognition of a variety of stress signals associated with tumours (36). The effect of γδ T cells and their anti-tumour function has been tested *in vivo* in clinical trials with the most potent N-BPs (zoledronate) either alone or in combination with low-dose interleukin 2 (IL-2), as IL-2 can enhance different effector functions of γδ T cells (29).

It has been shown that treatment with zoledronate stimulates γδ T cells more potently as well as it results in more IFN-γ production, which might have strong anti-tumour effects (37). Although these effects have been described for inducing high γδ T-cell expansion, in these trials zoledronate failed to induce large numbers of robust γδ T cells (29), (38). In another study it has been reported for the first time that the amount of Vγ9Vδ2 T cells and their production of tumour necrosis factor-α (TNF-α) and IFN-γ is decreased in melanoma patients and therefore indicative of immunodeficiency in these cancer patients. Therefore decreased number of γδ T cells may lead to lower immune defense against melanoma cancer cells (39). However, in another study it has been demonstrated that the impaired function of γδ T cells in patients with solid tumours could be restored by zoledronate activated Vγ9Vδ2 T cell-based immunotherapy (40).

The effect of N-BPs has been also tested in various different *in vitro* experiments. Castella *et al.* for example have reported that the treatment with zoledronate increased the sensitivity of myeloma and B cell lymphoma cells to Vγ9Vδ2 T cells (12).

Kunzmann *et al*. showed that pamidronate-treated γδ T cells mediate cytotoxicity against lymphoma (Daudi) and myeloma cell lines (RPMI 8226, U266). Furthermore, plasma cell survival was reduced from cultures derived from multiple myeloma patients by pamidronate-activated γδ T cells. The authors hypothesised that treatment with N-BPs might stimulate γδ T cells through the accumulation of IPP (41). This hypothesis was proved by Gober *et al.* who confirmed that N-BPs stimulate Vγ9Vδ2 T-cell activation through the accumulation of IPP (indirect pathway) rather than by structural homology with natural phosphoantigens [direct pathway, (42)].

2.6 Cytokines and costimulatory signals involved in γδ T-cell biology

Work from our group has shown that the depletion of isoprenoid pyrophosphates downstream of the mevalonate pathway results in inflammatory responses (*in vitro* and *in vivo*) by the IL-1 converting enzyme caspase-1, which cleaves pro-IL-1β and pro-IL-18 to generate the active cytokines IL-1β and IL-18 (2), (43). IL-1β is the predominant form of the cytokine IL-1 and is released mainly by monocytes and macrophages. IL-18, which was first identified to induce IFN-γ in immune cells, is also a member of the IL-1 cytokine family and is released by macrophages, DCs and keratinocytes (44), (45). The activation of caspase-1 not only influences IL-2 primed natural killer cells (NK cells), but also results in γδ T-cell activation (46). IL-18 has been shown to promote γδ T-cell expansion, which is stimulated by zoledronate and IL-2 (47). The cytokine IL-2, which was first identified as T-cell growth factor, is involved in the activation and proliferation of most T cells, NK cells and B cells (48). The granulocyte macrophage colony-stimulating factor (GM-CSF) is known to support DC development *in vitro* as well as to induce the differentiation in DCs from monocytes and human/mouse hematopoietic progenitor cells (49). IL-17 triggers the mobilization and expansion of neutrophils and is involved in regulation of inflammation and is produced by different cell types such as T helper cells (Th) 17, the third subset of Th cells, $CD8^+$ T cells, NK cells and γδ T cells (50). IL-17 further supports the *in vitro* production of the cytokines IL-1β and TNF-α as well as neutrophil chemoattractants.

In addition IL-17 is involved in intercellular adhesion molecule 1 (ICAM-1) expression and chemokine production (51).

Tsuda *et al.* suggested that $CD56^{bright}CD11c^{+}$ NK cells are involved in the IL-18 mediated effect during zoledronate-induced γδ T-cell expansion. IL-18 might have a stimulating effect on $CD56^{bright}CD11c^{+}$ cells, which correlates with efficient γδ T-cell expansion (52).

As mentioned before, phosphoantigens stimulate γδ T cells but it needs to be explored whether other receptors (beside the TCR) are involved in activation or if there are other signals or costimulatory factors, which promote TCR dependent expansion. The coreceptor CD27 for αβ TCR is also used to classify developmental stages. Thereby it has been shown that the CD70-CD27 interaction contributes to phosphoantigen induced γδ T-cell activation and has influence on their proliferation, survival and cytokine production (53). In addition, Vγ9Vδ2 T cells lack CD28, which is involved in αβ T-cell activation. However, it has also been shown that B7-CD28 interaction enhances the activation of γδ T cells (54).

3. Material and Methods

3.1 Material

3.1.1 Laboratory material and equipment

Centrifuges: *company*: Thermo Fisher Scientific; *model*: Sorvall RT-7 Plus and Thermo Sorvall RT 6000B

CO_2-Incubators: *company*: Thermo Fisher Scientific; *model*: Forma Water Jacketed CO_2 Incubator, 37°C, CO_2: 0.5%

Flow Cytometry: *company*: BD Bioscience; *model*: FACSCanto II; *software*: BD FACSDiva™ 6.1.2, BD FlowJo Version 7.2.5, FCAP Array 1.0.1

Laminar Flow Sterile Working Bank: *company*: LAF; *model*: VFRS 1206

Microscope: *company***:** Olympus; *model*: CK 2 INVERTED MICROSCOPE; equipped with a digital camera**:** *company*: Jenoptik; *model*: ProgRes CT3; *software*: ProgRes CapturePro 2.5

3.1.2 Isolation of peripheral blood mononuclear cells (PBMCs)

Product	Company	Stock concentration or stock volume	Volume	Order-No.
Heparin (15 U/ml)	Lovenox	40 mg per 0.4 ml ampule	195 µl	(pharmacy)
Ficoll (LSM 1077 Lymphocyte Separation Medium)	PAA	500 ml	90 ml	J15-004

Table 1: Material used for isolation of PBMCs

Buffer A per 500 ml flask:

Product	Company	Stock concentration or stock volume	Volume	Order-No.
HBBS	Lonza	500 ml	500 ml	BE10-527F
FBS (0.5 %)	HyClone	500 ml	2.5 ml	SH30070.03

Table 2: Components of buffer A

Buffer B per 500 ml flask:

Product	Company	Stock concentration or stock volume	Volume	Order-No.
PBS (without Ca^{2+}/Mg^{2+})	Lonza	500 ml	500 ml	BE17-516F
FBS (0.5 %)	HyClone	500 ml	2.5 ml	SH30070.03
EDTA (2 mM) Versen	BiochromeAG	1 % w/v	34 ml	L2113

Table 3: Components of buffer B

3.1.3 Cryo cell preparation

Freezing Container: *company*: Thermo Scientific; *model*: Nalgene® Mr. Frosty® Cryo 1°C Freezing Containers, *Order No.*: 5100-0001

Freezing media per cryotube 1 ml:

Product	Company	Stock concentration or stock volume	Volume	Order No.
RPMI 1640 (50 %)	Lonza	500 ml	500 µl	BE12-167F
FBS (40 %)	HyClone	500 ml	400 µl	SH30070.03
DMSO (10 %)	SIGMA	100 ml	100 µl	D2650-100ML

Table 4: Freezing media

3.1.4 Magnetic Activated Cell Sorting (MACS®)

Product	Company	Order-no.	Supplementary characteristics
MACS® Multi Stand	Milteny Biotec	130-042-303	
MACS® MIDI MACS Magnet	Milteny Biotec	130-042-302	
Isolation Columns (LS)	Milteny Biotec	130-042-401	
Depletion Columns (LD)	Milteny Biotec	130-042-901	
CD14 MicroBeads, human	Milteny Biotec	130-050-201	Isotype: mouse IgG2a
CD56 MicroBeads, human	Milteny Biotec	130-050-401	Isotype: mouse IgG1
HLA-DR MicroBeads, human	Milteny Biotec	130-046-101	Isotype:mouse IgG1
TCR γ/δ^+ T Cell Isolation Kit, human	Milteny Biotec	130-092-892	Isotype: mouse IgG1

Table 5: Material used for MACS®

MACS buffer (per 500 ml flask):

Product	Company	Stock concentration or stock volume	Volume	Order No.
PBS (without Ca^{2+}/Mg^{2+})	Lonza	500 ml	500 ml	BE17-516F
FBS (0.5%)	HyClone	500 ml	2.5 ml	SH30070.03
EDTA (2 mM) Versen	BiochromeAG	1% w/v	34 ml	L2113
Intratect (1:1000) human poly IgGs	Biotest	50 g/l	0.5 ml	624 050 030

Table 6: Components of the MACS buffer

3.1.5 Cell culture reagents, media and buffers

Product	Company	Stock concentration	Order No.	Supplementary characteristics
Caspase I Inhibitor V (YVAD)	ALEXIS	200 mM	260-016-M005	solved in DMSO
GGPP	Echelon	1.99 mM	I-0220	solved in A. dest.
Proleukin ® (IL-2)	Novartis	100.000 U/ml	(pharmacy)	solved in A. dest.
rhu IL-18	MBL	25 µg/ml	B-001-5	solved in A. dest.
Zoledronic acid monohydrate	Sigma-Aldrich	1 mg/ml (= 3.6 mM)	SML 0223-10MG	solved in A. dest.
rhu IL-1β/IL-1F2	R&D	5 µg/ml	201-LB	solved in PBS
Leukine® (GM-CSF)	Berlex	80.000 U/ml	(pharmacy)	solved in PBS

Table 7: Cell culture reagents

Cell culture media (RPMI plus 10% FBS per 500 ml flask):

Product	Company	Stock concentration or stock volume	Volume	Order No.
RPMI 1640	Lonza	500 ml	500 ml	BE12-167F
Hepes-buffer 10 mM	Lonza	1 M	5.5 ml	BE17-737E
FBS (10%)	HyClone	500 ml	50 ml	SH30070.03
GlutaMAX™	GIBCO	100 x	5.5 ml	35050-079
Na-Pyruvate	Lonza	100 mM	5.5 ml	BE13-115E
NEAA	Lonza	100 x	5.5 ml	BE13-114E
Penicillin/Streptavidin	PAA	100 x	5.5 ml	P11-010

Table 8: Cell culture media

Cell culture material

Product	Company	Order No.
PBS (without Ca^{2+}/Mg^{2+})	Lonza	BE17-516F
FBS	HyClone	SH30070.03
Trypan Blue (0.4% solution); sterile filtered	Sigma	T8154
Counting chamber (depth: 0.1 mm, Neubauer improved)	MARIENFELD	0640010
eFluor 780 (Fixable Viability Dye)	eBioscience	65-0865
Costar 96 well cell culture plates (round bottom with lid, tissue culture treated, nonpyrogenic, polystyrene, sterile)	Corning	3799

Table 9: Cell culture material

FACS-buffer (per 500 ml flask):

Product	Company	Stock concentration or stock volume	Volume	Order No.
PBS (without Ca^{2+}/Mg^{2+})	Lonza	500 ml	500 ml	BE17-516F
FBS (0.5%)	HyClone	500 ml	2.5 ml	SH30070.03
Intratect (1:1000) human poly IgGs	Biotest	50 g/l	0.5 ml (= 1:1000)	624 050 030

Table 10: Components of the FACS buffer

FIX- Buffer (1.85 % Formaldehyde solution per 500 ml flask):

Product	Company	Stock concentration or stock volume	Volume	Order No.
HBBS	Lonza	500 ml	475 ml	BE10-527F
FBS (0.5 %)	HyClone	500 ml	2.5 ml	SH30070.03
Formaldehyde solution	Merck	37 %	25 ml	8187081000

Table 11: Components of the FIX buffer

Flow cytometer reagents:

Product	Company	Order No.
BD FACSFlow™	BD Bioscience	342003
BD FACS™ Cleaning Solution	BD Bioscience	340345
BD FACS™ Shutdown Solution	BD Bioscience	334224

Table 12: Flow cytometer reagents (BD Bioscience FACSCanto II)

3.1.6 Antibodies

Product	Company	Volume/Test	Order No.	Supplementary characteristics
CD14-APC (mouse anti human)	BD Bioscience	1 µl	345787	Clone: MΦP9 Isotype: IgG2b
CD14-FITC (mouse anti human)	BD Bioscience	10 µl	345784	Clone: MΦP9 Isotype: IgG2b
CD25-PE (mouse anti human)	BD Bioscience	10 µl	341011	Clone: 2A3 Isotype: IgG1,k
CD27-APC (mouse anti human)	BD Bioscience	10 µl	558664	Clone: M-T271 Isotype: IgG1,k
CD3-Per-CP-Cy5.5 (mouse anti human)	BD Bioscience	10 µl	332771	Clone: SK7 Isotype: IgG1
CD56-APC (mouse anti human)	Beckman Coulter	10 µl	IM2474	Clone: N901 (NKH-1) Isotype: IgG1,k
CD56-PE (mouse anti human)	Beckman Coulter	10 µl	A07788	Clone: N901 (NKH-1) Isotype: IgG1,k
TCR Vδ2-FITC (mouse anti human)	Beckman Coulter	10 µl	PN IM1464	Clone: IMMU 389 Isotype: IgG1
IFN-γ-PE (intracellular staining)	BD Bioscience	10 µl	559327	Clone: B27 Isotype: IgG1

Table 13: Antibodies used for flow cytometric stainings

3.1.7 Cytometric Bead Array (CBA) material

Product	Company	Order No.
BD CBA Human Soluble Protein Master Buffer Kit	BD Bioscience	558264
BD Cytometer Setup & Tracking beads	BD Bioscience	641319
BD CBA Human IFN-γ - Flex Set	BD Bioscience	558269
BD CBA Human TNF – Flex Set	BD Bioscience	560112
BD CBA Human IL-2 - Flex Set	BD Bioscience	558270
BD CBA Human IL17-A – Flex Set	BD Bioscience	560383
BD CBA Human GM-CSF-Flex Set	BD Bioscience	558335
BD CBA Human IL-1β - Flex Set	BD Bioscience	558279

Table 14: CBA reagents

3.1.8 Enzyme-linked immunosorbent assay (ELISA)

Product	Company	Order No.
Human IL-18 ELISA Kit	MBL	Code No. 7620

Table 15: ELISA Kit for IL-18 measurements

3.1.9 Intracellular cytokines staining

Product	Company	Order No.
Brefeldin A (BFA) Solution	BD Bioscience	346049
FIX & PERM®	AN DER GRUB	GAS-002
Intratect (1:1000) human poly IgGs	Biotest	624 050 030
PBS (without Ca^{2+}/Mg^{2+})	Lonza	BE17-516F

Table 16: Products for intracellular cytokine staining

3.2 Methods

3.2.1 Isolation of peripheral blood mononuclear cells (PBMCs)

The buffy coats were kindly provided by the Central Institute of Blood Transfusion (University Hospital of Innsbruck). The PBMCs were isolated from buffy coats obtained from healthy donors, which gave written informed consent to use of their residual buffy coats, with approval from the University Hospital of Innsbruck Review Board.

At first 130 ml of buffer A (**Table 2**) were filled into a cell culture flask followed by adding 15 U/ml Heparin (195 µl Heparin). Then the blood (50 ml) was carefully transferred into the cell culture flask followed by cautious mixing. Next the diluted blood was gently layered (30 ml) onto 15 ml Ficoll in a 50 ml tube (altogether 6 tubes) and centrifuged (2300 RPM, 10 min, at RT, without a brake). After the centrifugation step the tubes were carefully removed from the centrifuge while not disturbing the layering. Then the PBMCs were isolated from the interphase (**Fig. 4**) of the Ficoll solution (between the erythrocytes and the plasma) and transferred into a new 50 ml tube up to the 25 ml graduation (altogether 3 - 4 tubes). Subsequently, the tubes were filled up with ice cold buffer B (**Table 3**) and centrifuged (1200 RPM, 10 min, 0 °C, with a brake). The supernatant was discarded down to the 7 ml graduation and the pellet resuspended. Subsequently the cells were collected in one tube by pipetting the resuspended cells from tube to tube. The empty tubes were rinsed by pipetting 5 ml of buffer B (**Table 3**) to recover all cells. In order to wash the cells the tube was filled with ice cold buffer B (**Table 3**) and centrifuged (1200 RPM, 10 min, 0°C, with a brake). The washing step was repeated until the supernatant was getting clear. Finally the pellet was resuspended in 30 ml of buffer A (**Table 2**) and the cell number was determined by Neubauer-counting chamber (stained in the appropriate volume with Trypan Blue solution 0.4 %).

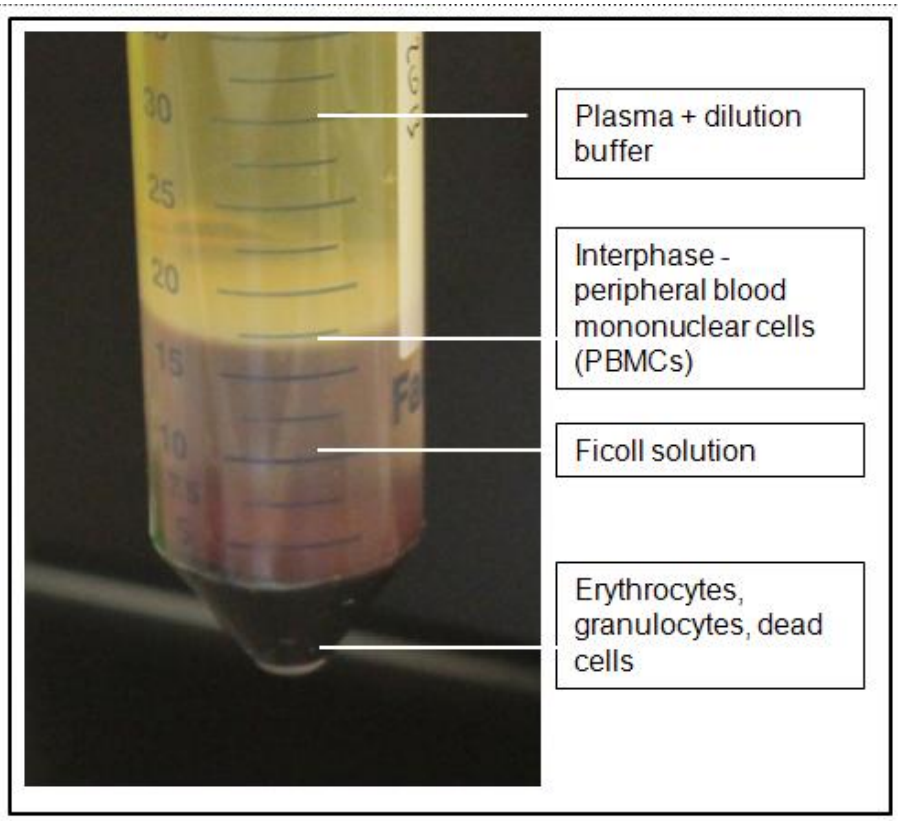

Figure 4: Scheme after first centrifugation step of PBMC preparation: *The interphase of the PBMCs is concentrated in barrier layer between the Ficoll solution and the plasma/buffer solution. (The picture was kindly provided by Hubert Gander).*

3.2.2 Cryopreservation

Freezing

The PBMCs were centrifuged, the supernatant discarded and the pellet resuspended in the freezing medium **(Table 4)** either with 100 x 10^6 cells/cryotube or 30 x 10^6 cells/cryotube**.** In the end the PBMCs were immediately frozen in a freezing container at -80 °C, which allows controlled rate of cooling (-1°C/minute). After a few days the PBMCs were finally stored in nitrogen liquid storage cell bank**.**

Thawing

The buffy coats (PBMC: 100 x 10^6 cells or 30 x 10^6), stored in nitrogen liquid storage cell bank, were thawed in a water bath at 37 °C. Next the cells were transferred into a 50 ml tube followed by rinsing the cryotube with PBS plus 0.5 % FBS to recover all cells. In order to get rid of the toxic DMSO the thawed cells were washed by dropwise adding PBS plus 0.5 % FBS into the tube containing the cell suspension up to the 15 ml graduation while gently shaking. The stepwise dilution of DMSO avoids the osmotic stress. Then the tube was immediately filled up with PBS plus 0.5 % FBS and centrifuged (1200 RPM, 10 °C) for 10 min. In the end the pellet was resuspended in the appropriate volume in cell culture media (**Table 8**) for the immune monitoring assay and the final cell number was determined by Neubauer-counting chamber (stained in the appropriate volume with Trypan Blue solution 0.4 %).
Note: In order to do a MACS® cell separation as fast as possible the cell number was determined at a volume of 15 ml. In the meantime the cells were filled up with PBS plus 0.5 % FBS and then centrifuged (1200 RPM, 10 °C) for 10 min followed by the steps of the MACS® cell separation [3.2.3 Magnetic Activated Cell Sorting (MACS®)].

3.2.3 Magnetic Activated Cell Sorting (MACS®)

CD14$^+$ cell isolation using MACS® cell separation

The CD14 MicroBeads are used for positive selection of human monocytes from PBMCs. Therefore the cells were centrifuged (1200 RPM, 10 °C) for 10 min, the supernatant aspirated and the pellet resuspended in MACS buffer (**Table 6**, 80 µl per 1 x 10^7 cells). Then the MicroBeads conjugated to monoclonal anti-human CD14 antibodies (20 µl per 1 x 10^7 cells) were added in a ratio of 4:1 and incubated for 20 min at 4 °C (light protected). Afterwards the cells were washed with 2 ml MACS buffer (**Table 6**) per 1 x 10^7 cells and centrifuged (1200 RPM, 10 °C, 10 min). The supernatant was aspirated and subsequently the pellet was resuspended to achieve a cell concentration of 1 x 10^8 cells (max. number of total cells 2 x 10^9) in 500 µl degassed, ice-cold MACS buffer (**Table 6**). Meanwhile the MACS Isolation Column (LS), which was placed with the column wings to the front into the magnetic field of the MACS Seperator, was calibrated by rinsing with 3 ml of the degassed, ice-cold MACS buffer (**Table 6**). After the buffer was run through the PBMC cells were applied to the prepared LS column. The empty tube was first rinsed with 500 µl ice-cold MACS buffer (**Table 6**) and then the recovered cells also applied to the LS column. The unlabeled cells pass through the column and were collected in a sterile 50 ml tube. The column was washed by adding 3 x 3 ml of the prepared degassed MACS buffer (**Table 6**), which were each time applied once the column reservoir was empty. After the last run-through the column was removed from the separator and was placed on a new collection tube. Finally, 6 ml of the MACS buffer (**Table 6**) were applied to the LS column and then the fraction with the magnetically labeled cells (CD14$^+$ cells) was flushed out by firmly inserting the plunger supplied with the LS column. In the end the cells were centrifuged (1200 RPM, 10 °C, 10 min), the supernatant was aspirated and the pellet resupended in cell culture media (**Table 8**) and stored on ice.

Note: A sample (~ 100.000 cells) of the isolated cells was collected for phenotype analysis on day 0 (3.2.5 Phenotypic analyses). The cell purity had to be >95% for further cell preparations.

HLA-DR$^+$ cell depletion using MACS® cell separation

All accessory cells (antigen presenting cells) were depleted using MicroBeads conjugated to monoclonal mouse anti-HLA-DR antibody and the MACS Depletion Column (LD) by the same procedure as described in the CD14$^+$ cell isolation section. In contrast, the cell depletion is performed with LD columns (max. number of labeled cells 1 x 10^8, max. number of total cells 5 x 10^8) instead of LS columns and the LD columns were calibrated by applying 2 ml of the degassed, ice-cold MACS buffer (**Table 6**). The column was washed by adding 2 x 1 ml of the prepared MACS buffer (**Table 6**) and the unlabeled cell fraction was collected as it contained the cells of interest (HLA-DR$^-$ cells) while labeled cells were retained in the LD column.

CD56$^+$ cell depletion using MACS® cell separation

The CD56$^+$ cells were depleted using MicroBeads conjugated to monoclonal anti-human CD56 antibodies and an LD column (max. number of labeled cells 1 x 10^8, max. number of total cells 5 x 10^8) by the same procedure as described in the HLA-DR$^+$ cell depletion section.

CD14$^+$ cell depletion using MACS® cell separation

The CD14$^+$ cells were depleted using MicroBeads conjugated to monoclonal anti-human CD14 antibodies and an LD column (max. number of labeled cells 1 x 10^8, max. number of total cells 5 x 10^8) by the same procedure as described in the HLA-DR$^+$ cell depletion section.

γδ T-cell isolation using MACS® cell separation

The TCR γ/δ$^+$ T-cell Isolation Kit was used to isolate untouched γδ T cells by depletion of non-TCR γ/δ$^+$ cells. Therefore the non-TCR γ/δ$^+$ cells were first labeled with a cocktail of biotin-conjugated monoclonal antibodies and then in a second step labeled with streptavidin MicroBeads.

The unlabeled γδ T cells pass through the column, whereas the labeled non-TCR γ/δ$^+$ cells were retained on the LS column (max. number of labeled cells 1 x 10^8, max. number of total cells 2 x 10^9)**.** In order to start the MACS® cell separation, PBMCs were centrifuged (1200 RPM, 10 °C) for 10 min, the supernatant was aspirated and the pellet was resuspended in MACS buffer (**Table 6**, 80 µl per 1 x 10^7 cells). Then the cocktail of biotin-conjugated monoclonal anti-human antibodies against antigens not expressed by γδ T cells (20 µl per 1 x 10^7 cells) was added in a ratio of 4:1 and incubated for 10 min at 4 °C (light protected). Afterwards the cells were washed with 2 ml MACS buffer (**Table 6**) per 1 x 10^7 cells and centrifuged (1200 RPM, 10 °C). Next the supernatant was aspirated and subsequently the pellet resuspended in MACS buffer (**Table 6**, 80 µl per 1 x 10^7 cells). Then the streptavidin MicroBeads (20 µl per 1 x 10^7 cells) were added in a ratio of 4:1 and incubated for 20 min at 4 °C (light protected) followed by the same procedure as described in the HLA-DR$^+$ cell depletion section

3.2.4 Cell culture and stimulation

The cell number was determined by Neubauer-counting chamber (stained in the appropriate volume with Trypan Blue solution 0.4 %) and subsequently diluted with cell culture medium (**Table 8**) for immune monitoring assays (total PBMCs, subset-depleted PBMCs [1.5 x 10^6/ml] and purified γδ T cells [5 × 10^4 cells/ml or 5 × 10^5 cells/ml]). The cells were stimulated with IL-2 (100 U/ml) plus zoledronate (10 µM, 30 µM) either alone or combined with GGPP (10 µM) in 96-well round-bottom plates (0.2 ml) and placed in a CO_2-incubator. Moreover some cultures were also treated with IL-18 (200 ng/ml), IL-1ß (5 ng/ml), caspase-1 inhibitor YVAD (200 µM) and IL-18 neutralising antibody (5 µg/ml). Every 2 - 3 days fresh IL-2 (100 U/ml) was added to the cultured cells. Depending on the cell growth the cell culture medium of the cultured cells had to be changed after 3 - 5 days. Therefore 100 µl of the supernatant were carefully harvested without disturbing the cell aggregation. The supernatant was either used for cytokine measurements or discarded. Then 100 µl of fresh cell culture medium (**Table 8**) containing fresh IL-2 to achieve a final IL-2 concentration of 100 U/ml were added to each well.

When the cells have reached a certain cell density, the cells were split by passaging 100 µl of the resuspended cells to another well. Finally 100 µl of fresh medium (**Table 8**) plus fresh IL-2 (final concentration 100 U/ml) were added to each well. For cytokine measurements the supernatants were harvested after 1 – 3 days by pipetting gently 100 µl/well without disturbing the pellet. Then the tubes were centrifuged (1200 RPM, 10 °C, 5 min) and carefully approximately 90 µl of the cell debris-free supernatant were transferred into a new tube. The supernatants were finally stored at – 20 °C for further analysis [3.2.6 Cytometric Bead Array (CBA)]. The different cellular growth was documented with an Olympus CK2 microscope equipped with a ProgRes CT3 digital camera and ProgRes CapturePro 2.5 software (Jenoptik).

3.2.5 Phenotypic analysis

The cultured cells were harvested by resuspending the cells per well and the cell number was determined by Neubauer-counting chamber (stained in the appropriate volume with Trypan Blue solution 0.4%). Both the freshly isolated cells (day 0) as well as cultured cells harvested at the time indicated were washed with PBS plus 0.5 % FBS (1200 RPM, 10 °C) for 10 min. The pellet was resuspended in 500 µl PBS and then treated with 1 µl of the 1:10 predilution (diluted with DMSO) of eFluor 780 Fixable Viability Dye (1:5000), tightly vortexed and incubated for 3 min at RT (ligtht-protected) followed by the next washing step with FACS buffer (**Table 10**, 1200 RPM, 10 °C) for 10 min. Subsequently the pellet was resuspended in 30 µl FACS buffer (**Table 10**) and the cells were stained with fluorochrome-conjugated monoclonal antibodies (according to the manufacturer) either with TCRVδ2, CD3, CD27, CD25, CD56 and/or CD14 for 30 min on ice (light-protected). Then the cells were washed again with FACS buffer (**Table 10**, 1200 RPM, 10 °C, 10 min) and then finally fixed by resuspending the pellet with 200 µl FIX-buffer (sterile filtered, **Table 11**). In the end the cells were analysed with a FACSCanto II flow cytometer and BD FACSDiva™ software.

3.2.6 Cytometric Bead Array (CBA)

Levels of cytokines (IFN-γ, IL-1ß, TNF-α, GM-CSF, CCL2 and IL-17-A) were determined on day 3 – 5 in culture supernatants using the Cytometric Bead Array (CBA) Human Soluble Protein Master Buffer Kit from BD Bioscience and CBA Human Cytokine Flex Sets. The protocol of the Instruction Manual of BD Cytometric Bead Array (CBA) Human Soluble Protein Master Buffer Kit was adapted.
First a TOP standard was prepared by transferring the lyophilized standard spheres from each analyte from the BD CBA Human Soluble Protein Flex Set in a polypropylene tube (e.g. 15 ml Falcon tube), which was labeled “TOP standard”. The standards were reconstituted with 4 ml of Assay Diluent and were equilibrated for 15 min (light-protected, at RT) followed by gentle mixing via pipetting. Then 10 tubes (12 x 75 mm) for a serial dilution were labeled and arranged in following order: Top Standard (Std.) 2500 (tube 1), Std. 1250 (tube 2), Std. 625 (tube 3), Std. 312 (tube 4), Std 156 (tube 5), Std. 80 (tube 6), Std. 40 (tube 7), Std. 20 (tube 8), Std. 10 (tube 9), Std. 0 (tube 10). First 300 µl of Assay Diluent were transferred to the tubes 2 – 10. In the second step a serial dilution was performed by transferring 300 µl of the TOP standard to tube 2 (Std. 1250) followed by thorough mixing via pipetting. The serial dilution was continued by transferring 300 µl of tube 2 (Std. 1250) to tube 3 (Std. 625) and so on continued making the serial dilution until tube 9 (Std. 10). As a negative control (tube 10 = ZERO standard, **Fig. 5**) served a tube, which only contained Assay Diluent (0 pg/ml).
Later on a master mix consisting of Capture Beads and Detection Reagent of each cytokine was prepared in a 15 ml tube. Therefore the number of tests of the experiment (standard, samples and diluted samples) had to be determined. In order to start the preparation of the master mix each Capture Bead Reagent stock vial had to be vortexed for at least 15 seconds to resuspend the beads thoroughly before transferring them. Then the total volume of diluted beads and total volume for Capture beads needed for the experiment was determined. Each sample required 25 µl of diluted beads and 0.5 µl of Capture beads.

The total volume of diluted beads can be calculated by multiplying 25 µl by the number of tests. The same calculation had to be made for the volume of Capture Beads, which was calculated by multiplying 0.5 µl by the number of tests. Then the volume of Capture Bead Diluent and Detection Reagent Diluent needed to dilute the beads was determined. Therefore, the volume of each bead tested was subtracted from the total volume of diluted beads needed to perform the assay.

Example for the whole calculation:

53 tests x 25 µl of diluted beads = 1350 µl
53 tests x 0.5 µl of each Capture Bead = 26.5 µl
1350 µl total volume of diluted beads – 26.5 µl for each bead (analyte) = volume of Capure Bead Diluent.
e.g.

- if testing one analyte: 1350 µl – (26.5 µl x 1) = 1323.5 µl Capture Bead Diluent
- if testing six analytes: 1350 µl – (26.5 µl x 6) =1166 µl Capture Bead Diluent

Then the Capture Bead Diluent and the Capture Beads were also transferred into a tube labeled with “Master Mix”.

Assay Preparation

Afterwards 50 µl of the master mix were transferred into each assay FACS-tube (10 x standard tubes plus sample tubes). Then 25 µl of each sample or 25 µl of the standard were added to the corresponding assay tube under gentle vortexing following by an incubation step of 3 hours at RT (light-protected). In the meantime the Wash Buffer (1 ml per test tube) was prepared by sterile filtering the buffer (0.2 µM) with a 60 ml injection syringe. After the incubation step, in order to wash the sample, 1 ml of the Wash Buffer were added to each sample tube and centrifuged for 7 min at RT (1300 RPM).The supernatant was carefully aspirated and discarded and 200 µl of the Wash Buffer were added in order to resuspend the pellet.

Just before being analysed the samples were vortexted for 3 – 5 seconds. The samples were analysed using FACSCanto II system, BD FACSDiva™ software. The final concentrations of the individual cytokines were determined with the FCAP Array 1.0.1 software from BD Bioscience.

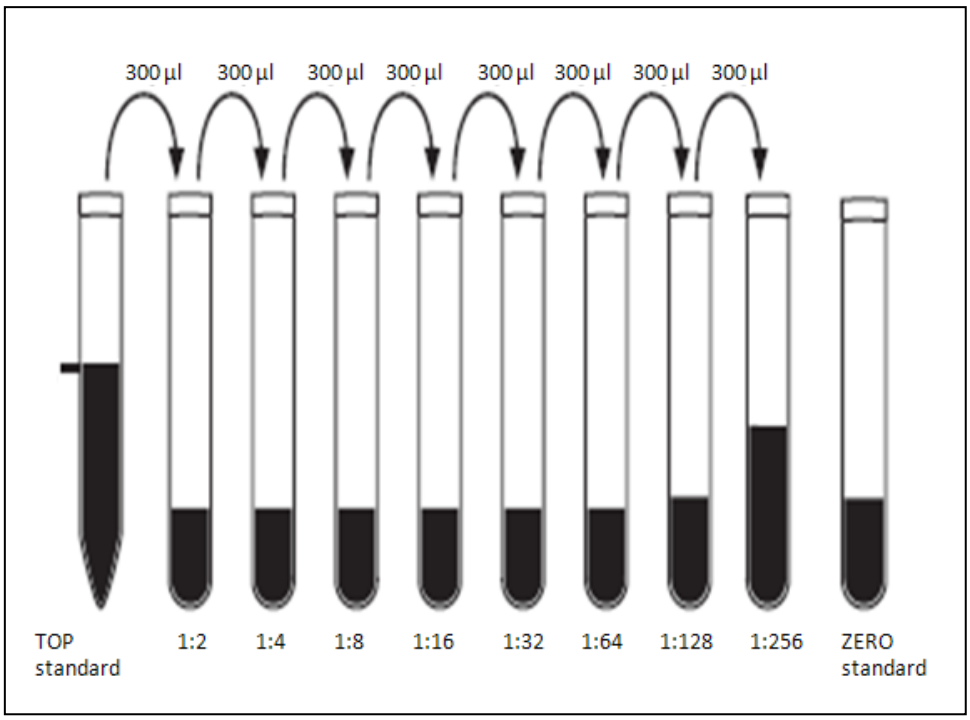

Figure 5: CBA - Concentration-row of standards: *First 300 µl of the TOP standard were pipetted in tube 2 thoroughly mixed via pipetting and then the same amount transferred to tube 3 and so on until tube 9 in order to prepare the serial dilution: TOP standard (tube 1), 1:2 (tube 2), 1:4 (tube 3), 1:8 (tube 4), 1:16 (tube 5), 1:32 (tube 6), 1:64 (tube 7), 1:128 (tube 8), 1:265 (tube 9) and zero standard (tube 10). [This figure was adapted from the Instruction Manual of BD Cytometric Bead Array (CBA) Human Soluble Protein Master Buffer Kit].*

3.2.7 ELISA

The levels of IL-18 were determined in culture supernatants using the Human IL-18 ELISA Kit from MBL based on the instruction manual.

3.2.8 Intracellular cytokine staining

The cells (1.5 x 10^6/ml) were cultured in cell culture medium (**Table 8**) and stimulated with IL-2 (100 U/ml) or IL-2 plus zoledronate (30 µM) and placed in a CO_2-incubator for 20 hours (day 1). During the last 3 – 4 hours the cells were treated with 10 µl 1:10 predilution of brefeldin A and finally harvested and washed with PBS plus 0.5 % FBS (300 g, 5 min, 4 °C). The pellet was resuspended in 500 µl PBS and then treated with 1 µl of the 1:10 predilution (diluted with DMSO) of eFluor 780 Fixable Viability Dye (1:5000), tightly vortexed and incubated for 3 min at RT (light-protected) followed by the next washing step with FACS buffer (**Table 10**). Subsequently the pellet was resuspended in 40 µl FACS buffer (**Table 10**) and the cells were stained for surface antigens with fluorochrome-conjugated monoclonal antibodies (according to the manufacturer's instructions) for TCRVδ2, CD3 and CD14 for 30 min on ice (light-protected), washed again with FACS buffer (**Table 10**, 300 g, 4°C, 5 min) and then fixed with 100 µl FIX-medium (reagent A) for 15 min (light-protected). After the incubation step the cells were washed twice with PBS (300 g, 4°C, 5 min). The pellet was resuspended in 100 µl PERM-medium (reagent B, 1:1000 with Intratect) and 20 µl of the fluorochrome-conjugated monoclonal anti-IFN-γ antibody (or antibodies against other cytokines) were added. After 20 min incubation at RT (light-protected) the cells were washed twice with PBS plus 0.5 % FBS (300 g, 4 °C, 5 min) and the pellet resuspended in 200 µl FIX buffer (**Table 11**). In the end the cells were analysed with FACSCanto II flow cytometer and BD FACSDiva™ 6.1.2 as well as with BD FlowJo Version 7.2.5 software.

3.2.9 Statistical analyses

For statistical analyses the experiments were always performed as duplicates or even sextuplicates and repeated at least two times. The Student t test was used to determine the group comparison for paired samples and the P values were statistically significant if they are equal to or less than 0.05. The experiment data were calculated using Microsoft Excel and SPSS software (SPSS Inc).

4. Results

The zoledronate-mediated inhibition of FPP synthase results in upstream accumulation of IPP and downstream deprivation of the prenyl pyrophosphates FPP and GGPP of the mevalonate pathway (**Fig. 3**). Previous studies have shown that the depletion of the isoprenoid pyrophosphates results in inflammatory responses. Caspase-1 subsequently cleaves pro-IL-1β and pro-IL-18 and provides bioactive forms of those cytokines, which amplify IFN-γ production (2). The caspase-1 inhibitor YVAD blocked the zoledronate-induced IFN-γ release in NK cells as well as in γδ T cells. Moreover, experiments with IL-18 costimulation have shown that this cytokine acts as a strong mediator during zoledronate-induced γδ T-cell expansion (55), (46), (2).

4.1 Phenotypic analyses of γδ T cells stimulated with zoledronate

As IL-2 is involved in T-cell activation and is expressed on activated lymphocytes (48) we first concentrated on the ligand-specific IL-2 receptor α chain (IL-2Rα, CD25) expression. Therefore we performed experiments with zoledronate treated PBMCs or with monocyte-depleted PBMCs ($CD14^-$ PBMCs) either alone or in combination with a neutralising antibody against endogenous IL-18. For phenotype analysis the cells were harvested after 20 hours and stained with anti-CD3, anti-Vδ2 and anti-CD25 antibodies.

In zoledronate-treated PBMCs, the expression of CD25 was induced. However, CD25 expression on the surface of γδ T cells was reduced by neutralization of endogenous IL-18. Subsequently, we depleted the monocytes ($CD14^+$ cells), as monocytes are known to be one of the sources of both IL-18 and IL-1β (56), (57). Depletion of $CD14^+$ cells reduced zoledronate-induced CD25 upregulation, however, addition of exogenous IL-18 to monocytes-depleted PBMCs resulted in enhanced CD25 expression (**Fig. 6**).

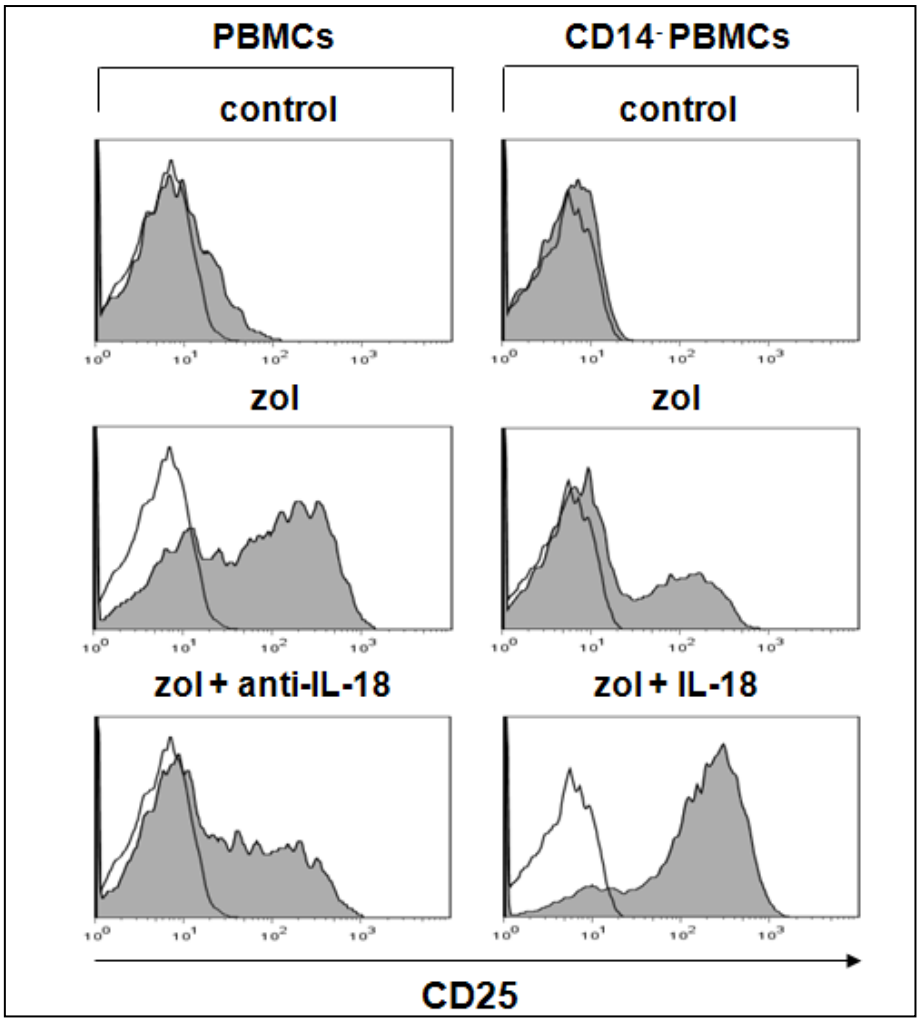

Figure 6: Upregulation of CD25 on γδ T cells by zoledronate-induced IL-18.

PBMCs (1.5 × 10^6/ml) were treated for 20 hours with zoledronate (30 µM) either alone or in combination with the neutralising antibody against endogenous IL-18 (5 µg/ml) in 96-well plates. The CD14$^-$ PBMCs were stimulated for 20 hours with zoledronate (30 µM) either alone or in combination with recombinant IL-18 (200 ng/ml). All cells were stained for CD3, TCRVδ2 and CD25. The cells were measured by flow cytometry and finally the Vδ2$^+$ T cells were gated and selectively analysed for CD25 expression (CD25 expression: filled histogram, isotype control: open histogram, zol: zoledronate) with the BD FACSDiva™ software.

4.2 Analyses of cytokine response

The release of IL-18 in response to stimulation of zoledronate was studied in $CD14^+$ PBMCs by ELISA. IL-2 enhances the IL-18 effect, which is known for its stimulating activity of IFN-γ production (44), (45). Therefore experiments were performed with $CD14^+$ PBMCs either without stimulation or with IL-2 and zoledronate treated cells each alone or combined with GGPP or YVAD, which is a specific inhibitor of caspase-1 (58). As shown in Fig. 7 zoledronate induced IL-18 secretion at low level. IL-2 alone had no effect. In presence of GGPP, which might restore protein prenylation, IL-18 was not detectable. The bio active form of IL-18 is generated by caspase-1, which can be inhibited by YVAD (58). In the presence of YVAD no IL-18 production was measured. The DMSO solvent control showed no effect (**Fig. 7)**.

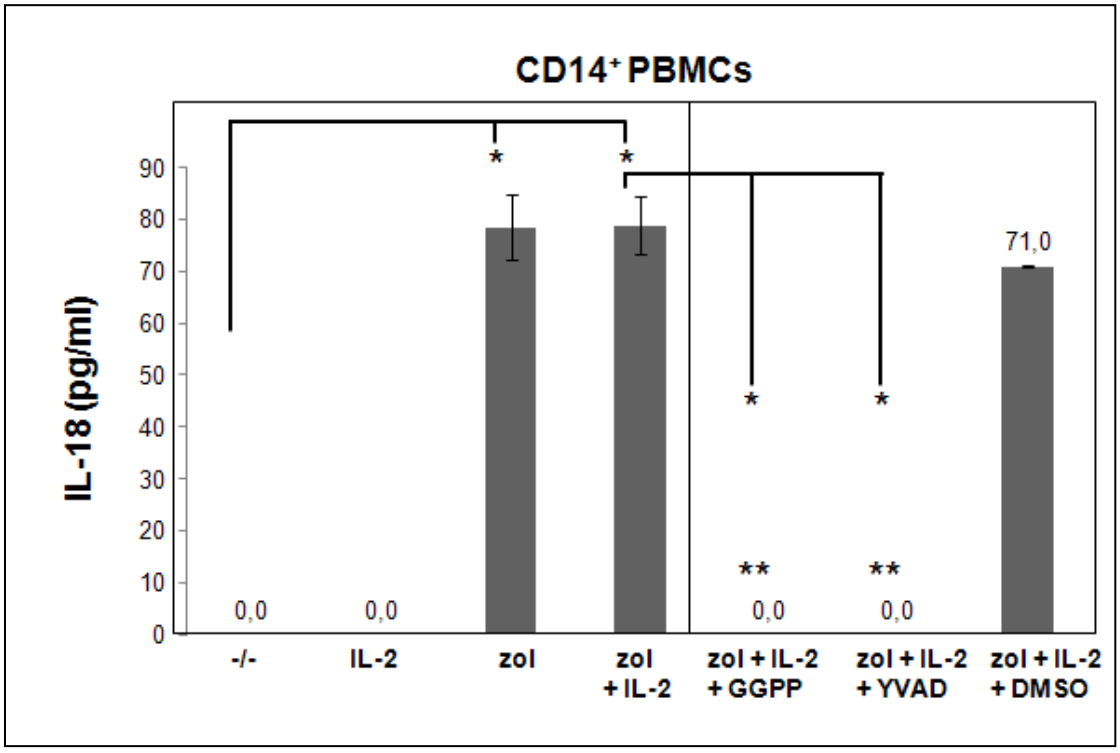

Figure 7: Addition of GGPP and YVAD abolished IL-18 secretion in $CD14^+$PBMCs. *$CD14^+$PBMCs (1×10^6/ml) were either left unstimulated or treated for 20 hours with zoledronate (30 µM) and IL-2 (100 U/ml) either alone or in combination with GGPP (10 µM) or caspase-1 inhibitor YVAD (200 µM).*

*The DMSO treated cells in combination with zoledronate + IL-2 served as a solvent control for YVAD. IL-18 was analysed from culture supernatants by ELISA. In Fig. 7 one experiment, which is representative of three independent experiments, is presented. The error bars are SD. * p < 0.05, zol: zoledronate.* ***Copyright 2013. The American Association of Immunologists, Inc.***

We further conducted experiments with two different donors, which have either low (0.6%) or high (10%) γδ T cell frequencies. Therefore PBMCs or monocyte-depleted PBMCs (**Fig. 8**) were stimulated with IL-2 either alone or in combination with zoledronate as it is described that the induction of IFN-γ by IL-18 is enhanced in combination with IL-2 (45). The cells were incubated for 20 hours in a CO_2-incubator and finally stained for the surface marker CD3 and for intracellular IFN-γ. In the absence of monocytes ($CD14^+$ cells) the production of intracellular IFN-γ was reduced or abrogated (**Fig. 9**).

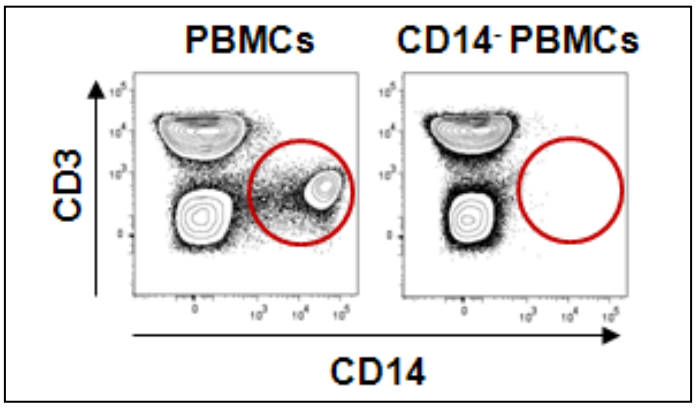

Figure 8: Flow cytometric control of depleted monocytes ($CD14^+$). *$CD14^+$ cells were depleted from PBMCs and stained for CD3 and CD14, checked on day 0 by flow cytometry.* ***Copyright 2013. The American Association of Immunologists, Inc.***

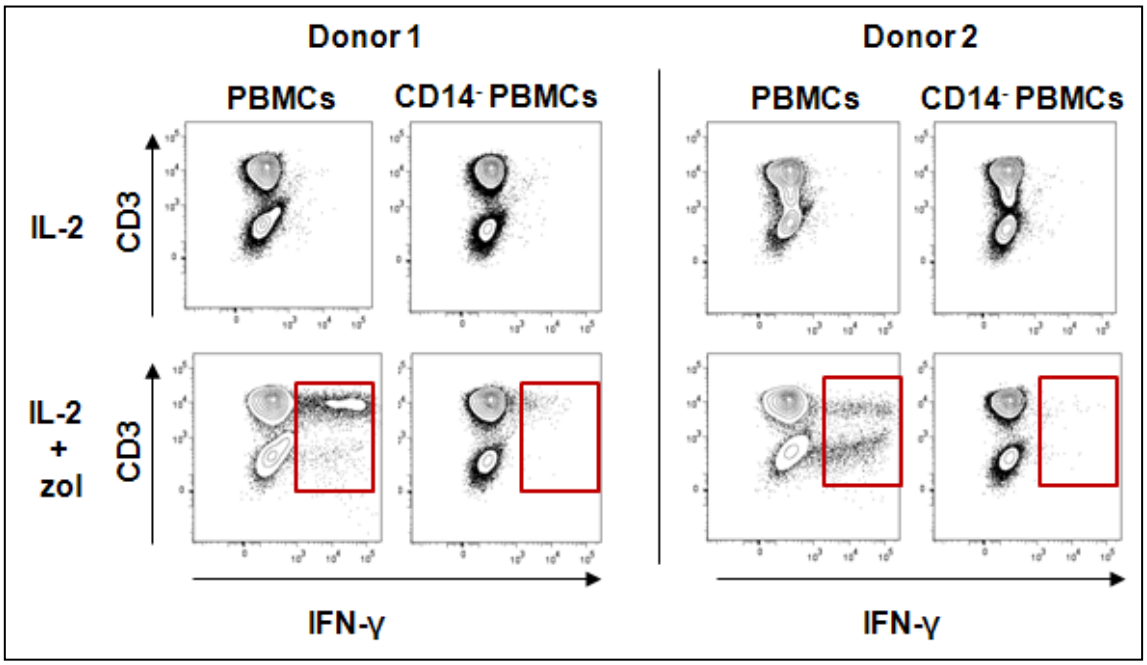

Figure 9: The early IFN-γ response induced by zoledronate plus IL-2 depends on monocytes. *Two different donors either with high (donor 1: 10%) or low (donor 2: 0.6%) γδ T cells starting frequency were examined for intracellular IFN-γ staining. Therefore PBMCS (1.5 x 10^6/ml) or monocyte-depleted PBMCs (CD14$^-$PBMCs, 1.5 x 10^6/ml) were treated with IL-2 (100 U/ml) either alone or in combination with zoledronate (30 µM) in 96-well plates. The cells were incubated for 20 hours in a CO_2-incubator, stained for intracellular IFN-γ and surface CD3 and finally measured with FACS Canto II flow cytometer, zol: zoledronate.*

We further performed experiments with PBMCs or with monocyte-depleted PBMCs (CD14$^-$ PBMCs). The cells were stimulated with IL-2 or zoledronate either alone, or both together in combination or without IL-18 neutralising antibody. Followed by a 20 hours incubation period, culture supernatants were harvested and analysed by CBA flex sets.

We have observed that zoledronate together with IL-2 induced an early cytokine response (IFN-γ, TNF-α, GM-CSF, IL-1ß), whereas after depletion of monocytes no or low amounts of cytokines were measured ($p < 0.01$). We also found that the monocyte chemoattractant protein-1 (MCP-1) was also induced by zoledronate treatment. MCP-1 is also referred to as chemokine (C-C motif) ligand 2 (CCL2) to attract monocytes, neutrophils, T cells and NK cells (59), (60). However, as in Fig. 10 demonstrated, the chemokine CCL2 upregulation is dependent on monocytes. The treatment of zoledronate plus IL-2 in combination with IL-18 neutralising antibody reduced the production of each analysed cytokine (**Fig 10**).

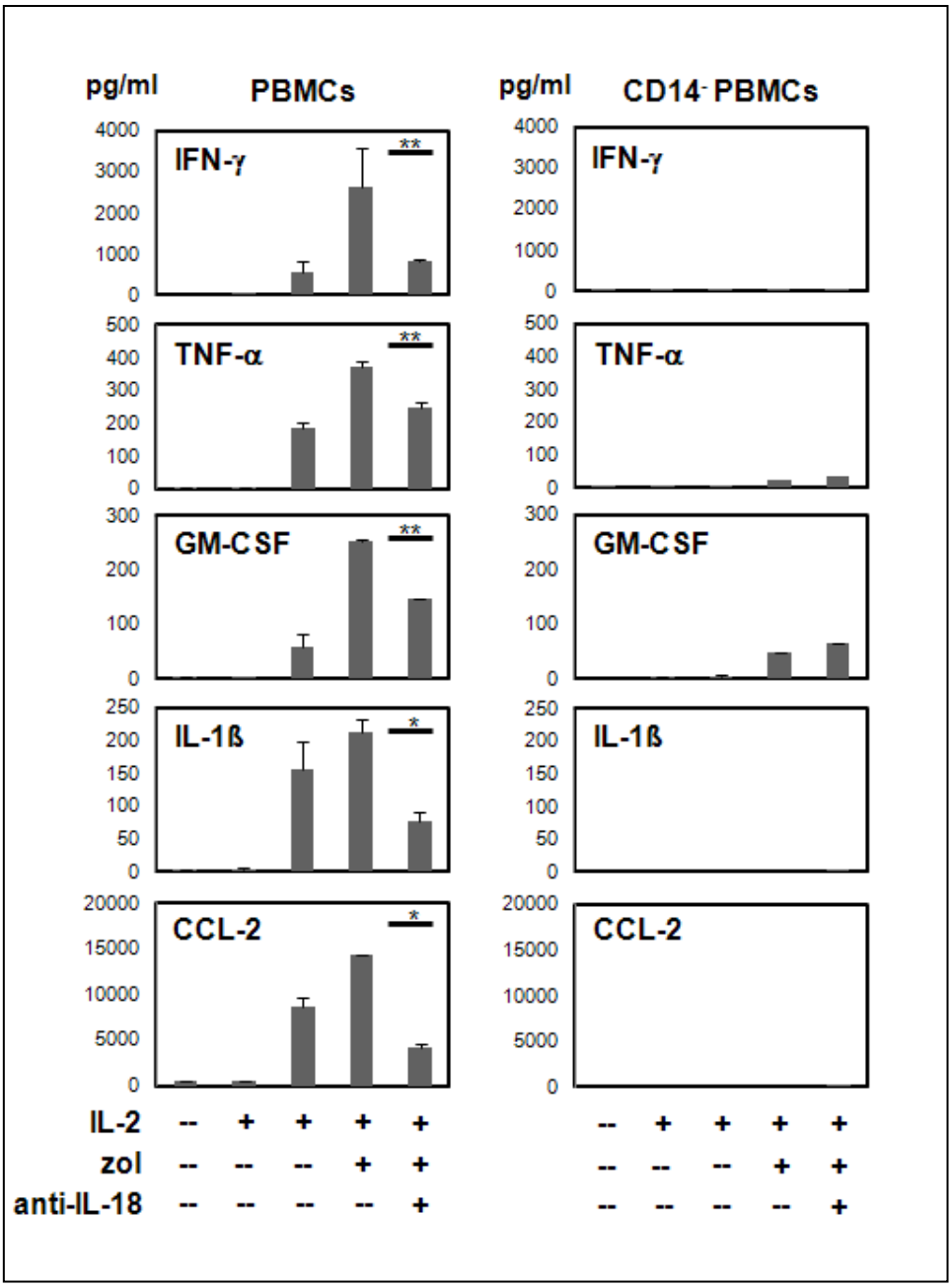

Figure 10: Early cytokine response in PBMCs induced by zoledronate treatments. *PBMCs (1.5 x 10^6/ml) or monocyte-depleted CD14$^-$PBMCs (1.5 × 10^6/ml) were stimulated for 20 hours either with IL-2 (100 U/ml) alone or in combination with zoledronate (30 µM) alone or combined with IL-18 neutralising antibody (5 µg/ml). The upregulation of the different cytokines was analysed in culture supernatants using CBA flex sets. In Fig. 10 one experiment, which is representative of three independent experiments, is presented.*

*The error bars are SD. * p < 0.05, ** p < 0.01, zol: zoledronate.* ***Copyright 2013. The American Association of Immunologists, Inc.***

4.3 Analysis of γδ T-cell proliferation

Compared to the cytokine response and CD25 upregulation, which occurred within the first 20 hours, the γδ T-cell expansion was delayed. Kinetic experiments demonstrated that γδ T-cell proliferation does not start until day 4 to day 5 (**Fig. 12**). Furthermore the delay was further increased when the monocytes were depleted. The delay of zoledronate could be explained by zoledronate-mediated inhibition of FPP synthase leading to downstream depletion of prenyl pyrophosphates, which serve as donor substrates for prenylation (2), (3). Further experiments have demonstrated that GGPP seems to be the main target of zoledronate-induced deprivation of prenyl pyrophosphates (46). Therefore we examined kinetic experiments with PBMCs and monocyte-depleted PBMCs ($CD14^-$PBMCs, **Fig. 11**), which were stimulated with zoledronate plus IL-2 either alone or in combination with GGPP. γδ T-cell proliferation was analysed on day 1, day 3, day 5 and day 7 of incubation. It was shown that addition of GGPP (10 µM), which is described as a poor antigen [300-fold less potent than the antigen IPP (10)], resulted not only in a higher proliferation but also in an earlier start of γδ T-cell expansion (**Fig. 12**).

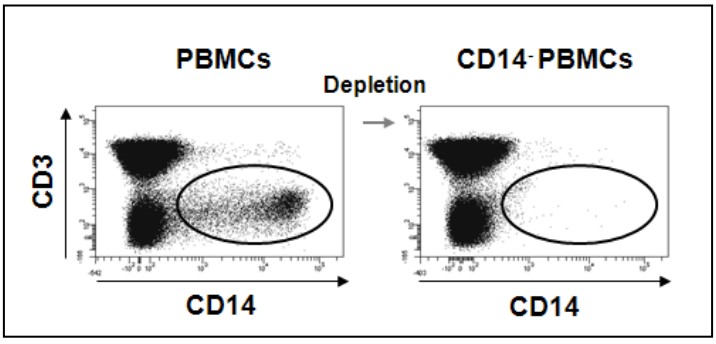

Figure 11: Flow cytometric control of depleted monocytes ($CD14^+$). *$CD14^+$ cells were depleted from PBMCs and stained for CD3 and CD14, checked on day 0 by flow cytometry.* ***Copyright 2013. The American Association of Immunologists, Inc.***

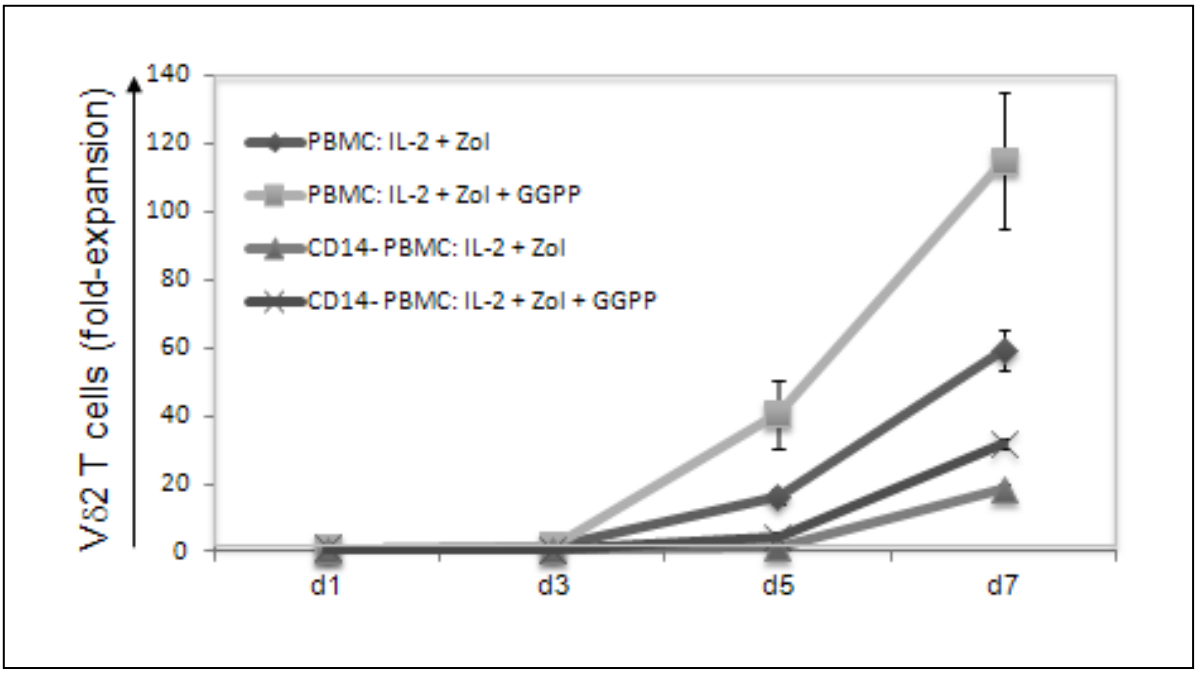

Figure 12: Addition of GGPP leads to earlier start of γδ T-cell- expansion and to a higher proliferation rate. *The kinetic experiment was performed with PBMCs (1.5 × 10^6/ml) and monocyte-depleted (CD14$^-$) PBMCs (1.5 × 10^6/ml) in 96-well plates. The cells were treated with zoledronate (10 µM) + IL-2 (100 U/ml) either alone or in combination with GGPP (10 µM). The cells were either stained on day 1, day 3, day 5 or day 7 for surface CD3 and TCR-Vδ2 and the γδ T-cell expansion was determined by flow cytometry. The cells were analysed by the BD FACSDiva™ software. The total numbers of γδ T cells in the individual cell cultures were derived from absolute cell numbers considering γδ T-cell frequency and used to quantify γδ T-cell expansion, zol: zoledronate.* ***Copyright 2013. The American Association of Immunologists, Inc.***

4.4 The role of accessory cells in zoledronate-induced γδ T-cell activation

γδ T cells recognise antigens without the requirement of APCs, e.g. DCs (27). Nevertheless, it is still not known if γδ T cells require costimulations, which are induced by APCs. In order to examine the role of accessory cells in IL-18 stimulated γδ T cells we designed experiments with cell cultures depleted of all accessory cells including monocytes, DCs, B cells and activated T cells. Moreover, as previous studies have shown that IL-18-mediated proliferation of γδ T cells might have effects on $CD56^{bright}$ NK cells (52), also $CD56^{+}$ cells were also depleted (**Fig. 13**). The cells were stimulated with IL-2 plus zoledronate in combination with the pyrophosphate GGPP either alone or in combination with IL-18 for 7 days. Finally, the cells were stained for surface CD3 and TCR-Vδ2. The loss of γδ T-cell proliferation (expansion factors < 0.13-fold) in $HLA\text{-}DR^{-}CD56^{-}$ PBMCs was due to the toxic effects of zoledronate, which can be prevented by addition of GGPP. The stimulation of GGPP in combination with IL-18 showed a strong induction of γδ T-cell proliferation (expansion factor >30 fold), which was not achieved by stimulation with GGPP alone (expansion factors of 1.3 fold). The expansion of γδ T cells was also achieved independently of $CD56^{+}$ cells, which leads to the conclusion that IL-18 stimulates γδ T cells directly. In addition, the less effective expansion in the presence of $CD56^{+}$ cells may be due to IL-18-mediated activation of NK-cell cytotoxicity (**Fig. 14**).

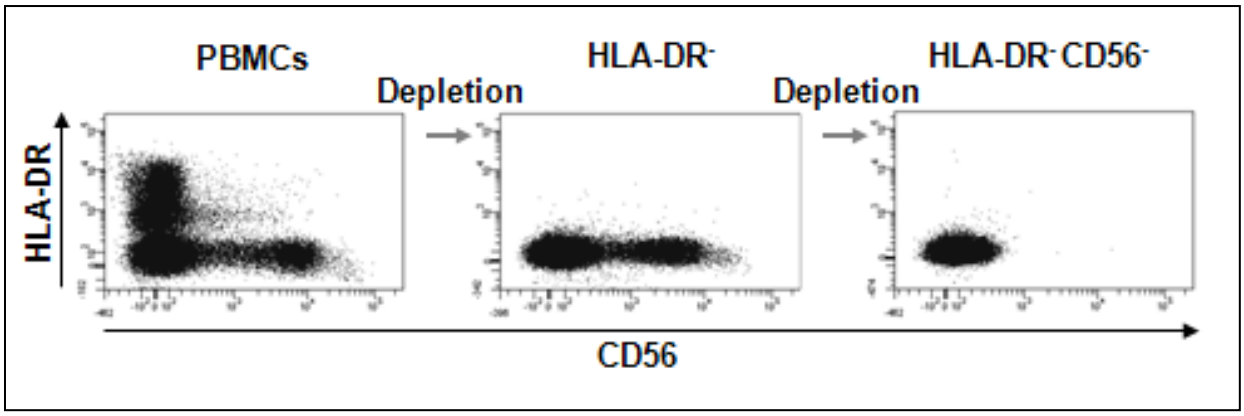

Figure 13: Flow cytometric control of PBMC subset depletion. *PBMCs were depleted either of HLA-DR$^+$ cells or of HLA-DR$^+$CD56$^+$ cells. The cells were stained for surface HLA-DR and CD56 and the purification was checked on day 0 by flow cytometry.* ***Copyright 2013. The American Association of Immunologists, Inc.***

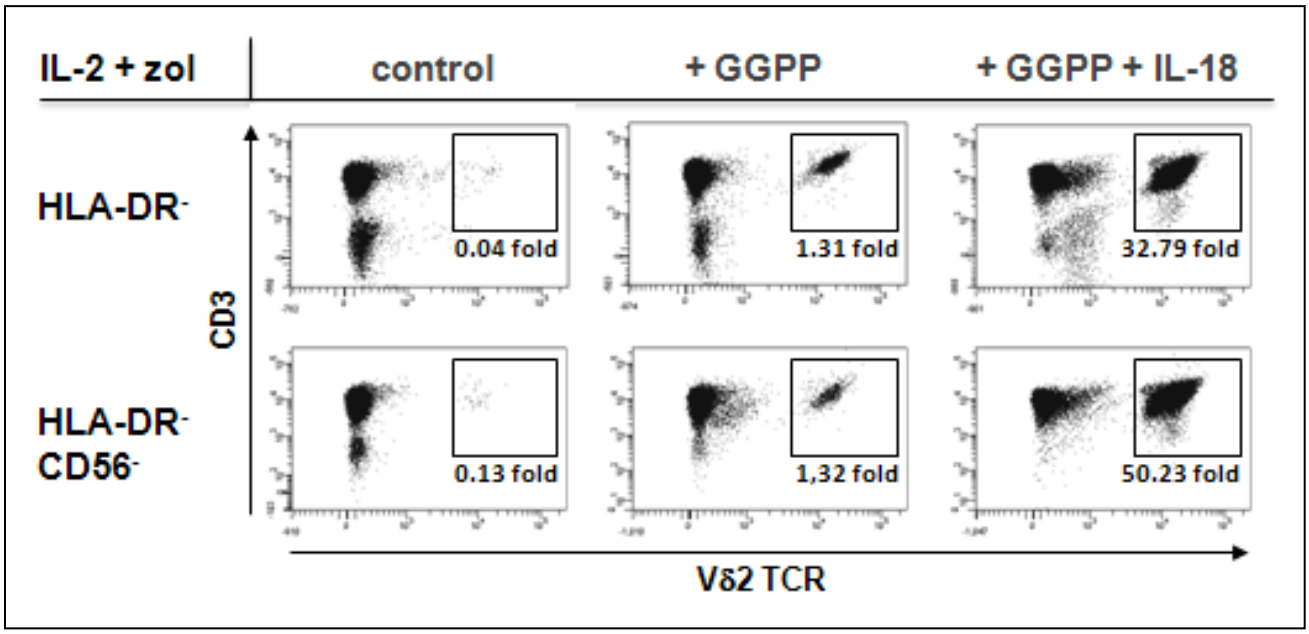

Figure 14: Addition of GGPP and IL-18 enhances the expansion of zoledronate plus IL-2 mediated γδ T cell expansion in the absence of any other accessory cells. *All accessory cells (HLA-DR$^+$) and NK cells (CD56$^+$) were depleted.*

The cells (1.5 x 10^6/ml) were stimulated in 96-well plates with zoledronate (10 µM) + IL-2 (100 U/ml) in combination with GGPP (10 µM) either alone or in combination with IL-18 (200 ng/ml). As a control HLA-DR$^-$ and HLA-DR$^-$CD56$^-$ cells were stimulated with IL-2 + zoledronate without other stimulation components. On day 7 the cells were stained for surface CD3 and TCR-Vδ2 and γδ T-cell expansion was determined by flow cytometry and the cells were analysed by the BD FACSDiva™ software. The total numbers of γδ T cells in the individual cell cultures were derived from absolute cell numbers considering γδ T-cell frequency and used to quantify γδ T-cell expansion, zol: zoldronate.

Moreover, the several cellular growth of the HLA-DR$^-$ PBMCs or HLA-DR$^-$CD56$^-$ PBMCs was documented on day 7 and it was shown that in the presence of zoledronate and IL-2 the cells did not aggregate and no expansion of γδ T cells could be observed (**Fig. 15**).

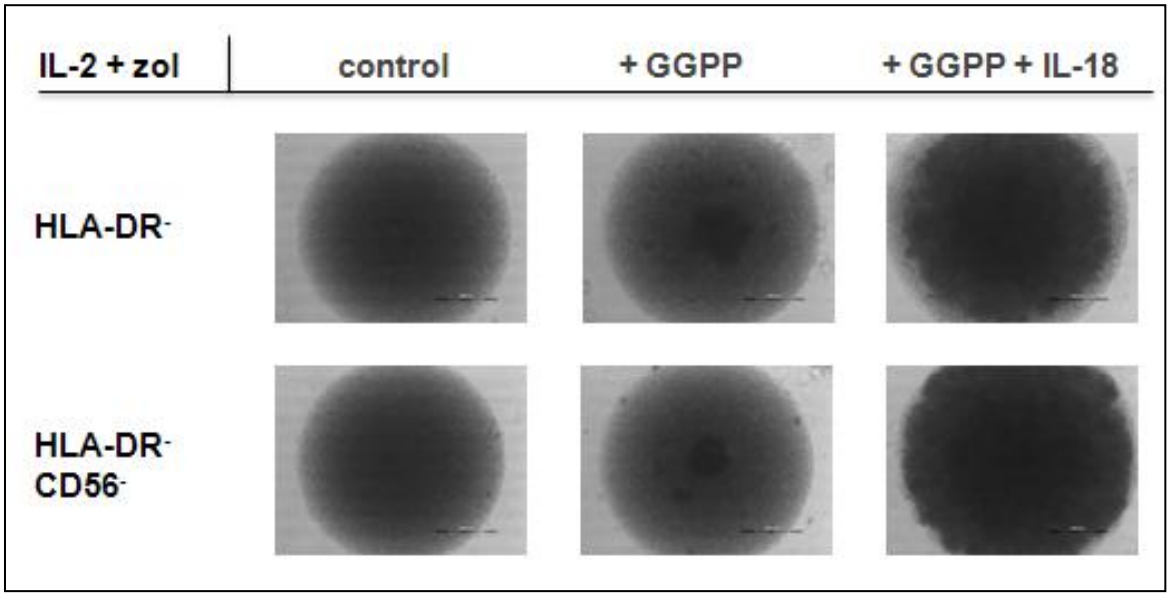

Figure 15: Different cell aggregation of HLA-DR$^-$ and HLA-DR$^-$CD56$^-$ cells.

All accessory cells (HLA-DR$^+$) and NK cells (CD56$^+$) were depleted.The cells (1.5 x 10^6/ml) were stimulated with zoledronate (10 µM) + IL-2 (100 U/ml) in combination with GGPP (10 µM) either alone or in combination with IL-18 (200 ng/ml).

As a control HLA-DR$^-$ and HLA-DR$^-$CD56$^-$ cells were stimulated with IL-2 + zoledronate without other stimulation components. The different cellular growth was documented with an Olympus CK2 microscope (magnification: 4×10) equipped with a ProgRes CT3 digital camera and ProgRes CapturePro 2.5 software (Jenoptik) The scale bar is 500 µm, zol: zoledronate.

Previous studies have revealed that CD56$^+$ γδ T cells show a higher resistance to Fas-ligand-mediated apoptosis as well as chemically-induced apoptosis and to be more cytotoxic, have stronger antitumour effects (61). We therefore also studied the CD56 expression on γδ T cells by staining the cells for CD3, TCR-Vδ2 and CD56. This led to the finding that treating with IL-18 enhanced the number of CD56$^+$ γδ T cells (**Fig 16**).

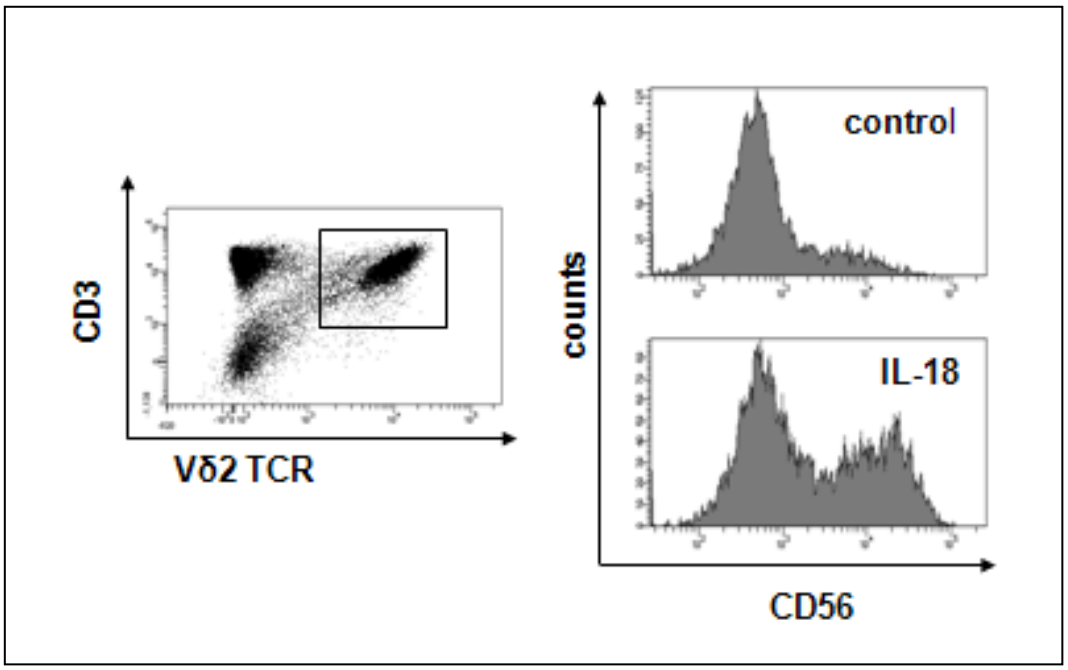

Figure 16: IL-18 enhanced the CD56 expression on γδ T cells. *PBMCs (1.5 x 10^6/ml) were stained on day 5 for CD3 and TCR-Vδ2 and surface CD56.*

The cells were examined by FACS Canto II flow cytometry and finally the Vδ2$^+$ T cells were gated and selectively analysed for CD56 expression by the BD FACSDiva™ software. ***Copyright 2013. The American Association of Immunologists, Inc.***

4.5 Expansion of highly purified γδ T cells

Previous experiments (**Fig. 14**) have shown that γδ T-cell expansion, induced by zoledronate plus IL-2 required no APCs when GGPP and IL-18 were present. Hence, we designed experiments with γδ T cells highly purified by negative isolation (**Fig. 17**). Highly purified γδ T cells were treated with IL-2 plus zoledronate either with GGPP alone or in combination with IL-18 costimulation. The toxic effect of zoledronate was measured by incubating the cells with eFluor 780 Fixable Viability Dye and analysed by flow cytometry. Only 8.6 % of the cells were viable after zoledronate treatment, however, supplementation with GGPP resulted in a much higher viability (> 75%). The effect of IL-18 in combination with GGPP slightly raised the cell viability to > 79% (**Fig. 18**).

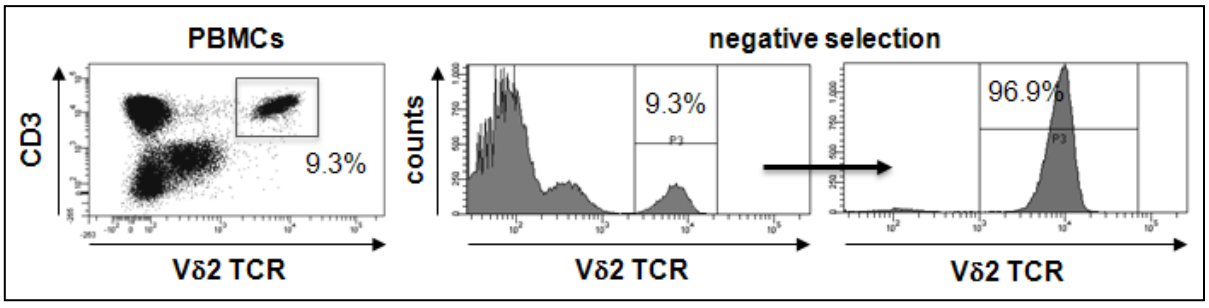

Figure 17: Flow cytometric control of highly purified γδ T cell. *γδ T cells were highly purified from PBMCs by negative selection. The cells were stained for CD3 and Vδ2 and the purification checked on day 0 by flow cytometry. The cells were finally analysed with the BD FACSDiva™ software.* ***Copyright 2013. The American Association of Immunologists, Inc.***

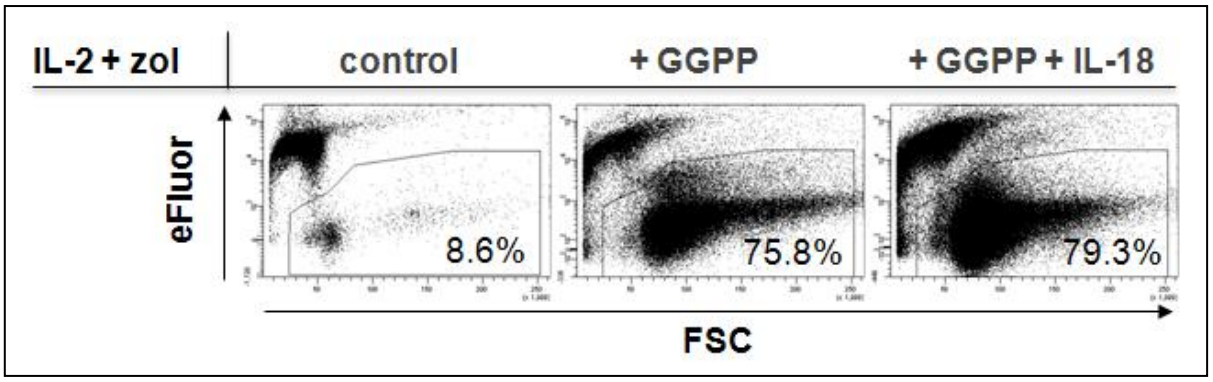

Figure 18: Supplementation with GGPP and IL-18 resulted in a much higher viability of highly purified γδ T cells. *γδ T cells were highly purified from PBMCs by negative selection. The cells (10^5 cells per 96 well) were treated with zoledronate (10 µM) + IL-2 (100 U/ml) either with GGPP (10 µM) alone or in combination with IL-18 (200 ng/ml). Zoledronate toxicity was analysed using eFluor 780 Fixable Viability Dye, which irreversibly labels dead cells. Finally, the cells were determined by flow cytometry. In the end, the cells were analysed by BD FACSDiva™ software. The viable cells exclude eFluor and increase the forward scatter (FSC) during activation, zol: zoledronate.* ***Copyright 2013. The American Association of Immunologists, Inc.***

Additionally, the cell growth of the highly purified γδ T cells was documented on day 3 and day 6. Thereby it was shown that the cell aggregation of the γδ T cells was enhanced by addition of GGPP on day 3 and was increased on day 6 **(Fig. 19)**. Moreover, the supplementation with IL-18, showed little influence on the cell viability **(Fig. 18)**, but highly boosted the γδ T-cell proliferation, also in a time-dependent-way. On day 7 the cells were stained for CD25. Stimulation with IL-18 induced an enhanced expression of CD25 on their cell surfaces **(Fig. 19)**.

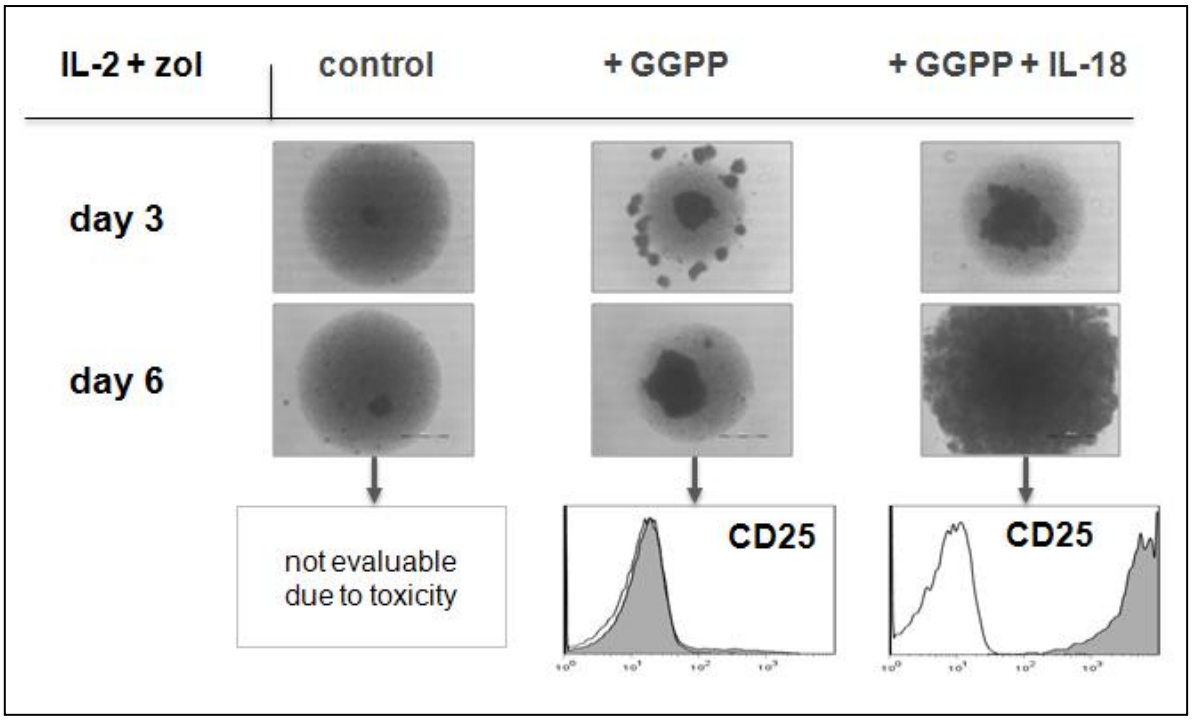

Figure 19: IL-18 enhances the γδ T-cell aggregation time-dependently and generated γδ T cells with high CD25 expression. *Highly purified γδ T cells (10^5 per 96 well) were stimulated with zoledronate (10 µM) + IL-2 (100 U/ml) in combination with GGPP (10 µM) either alone or in combination with IL-18 (200 ng/ml). As a control served γδ T cells, which were stimulated with IL-2 + zoledronate without other stimulation components. The different cell aggregation was documented on day 3 and day 6 with an Olympus CK2 microscope (magnification: 4×10) equipped with a ProgRes CT3 digital camera and ProgRes CapturePro 2.5 software (Jenoptik) The scale bar is 500 µm, zol: zoledronate. The γδ T cells were stained for surface CD25 on day 7 and analysed by flow cytometry using BD FACSDiva™ software. CD25 expression: filled histogram, isotype control: open histogram, zol: zoledronate.*

In order to analyse the time-dependent upregulation of CD25 we performed kinetic experiments with PBMCs. The cells were stimulated with IL-2 plus zoledronate in combination with GGPP either alone or in combination with IL-18. The cells were stained for CD25 on day 2, day 4, day 7 and were analysed using flow cytometry.

Whereas GGPP had no visible influence on CD25 expressing γδ T cells, IL-18 strongly enhanced the time-dependent upregulation of CD25 (**Fig. 20**).

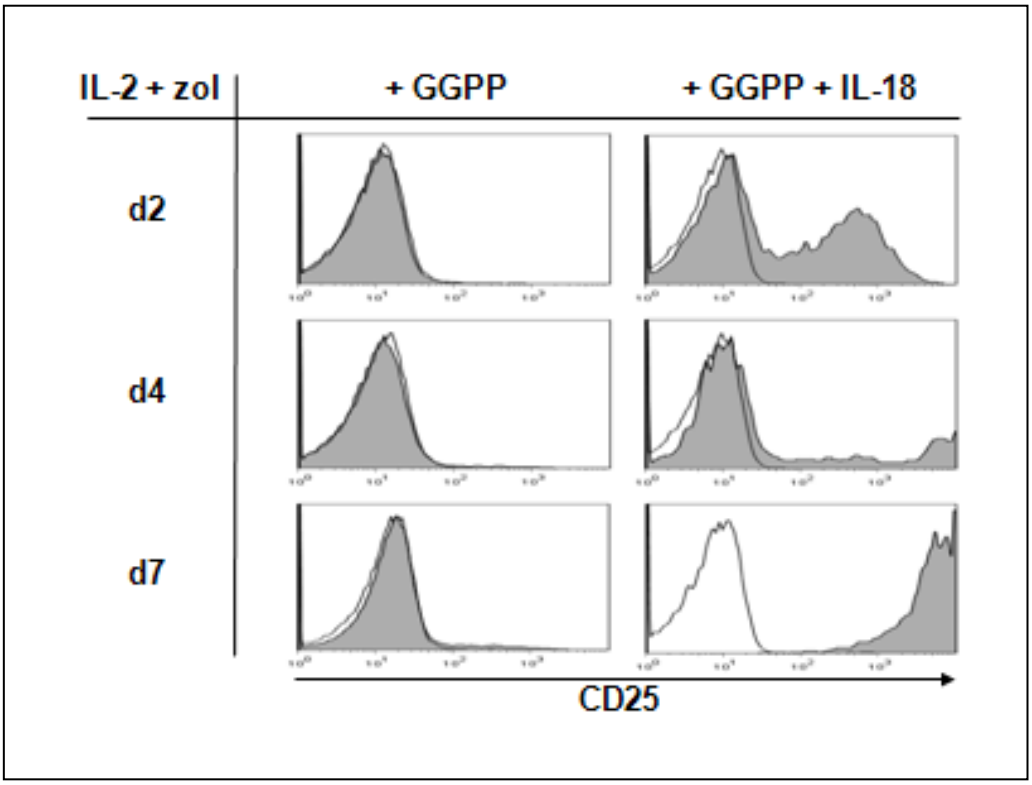

Figure 20: Time-dependent generation of γδ T-cell expressing high levels of CD25 by IL-18 stimulation. *PBMCs (1.5 x 10^6/ml) were stimulated with zoledronate (10 µM) + IL-2 (100 U/ml) in combination with GGPP (10 µM) either alone or in combination with IL-18 (200 ng/ml). For phenotype analysis the γδ T cells were stained for CD25 on day 2 (d2), day 4 (d4), day 7 (d7) and measured by FACS Canto II flow cytometer. Finally, Vδ2$^+$ T cells were gated and selectively analysed for CD25 expression (CD25 expression: filled histogram, isotype control: open histogram, zol: zoledronate) with the BD FACSDiva™ software.*

We further determined the different expansion of pure γδ T cells. The cells were treated with zoledronate plus IL-2 in combination with GGPP either alone or in combination with IL-18 costimulation. As a control γδ T cells were treated with zoledronate plus IL-2. The cells were stained on day 10 and the factor of expansion was calculated. The γδ T-cell expansion from γδ T cells, which were treated with zoledronate plus IL-2, was not evaluable due to the toxicity of zoledronate. However, in combination with the prenyl pyrophosphate GGPP, abrogating the toxic effect of zoledronate, γδ T-cell proliferation was enhanced (expansion < 4-fold). In combination with GGPP and by costimulation with IL-18, the γδ T-cell proliferation was strongly amplified (expansion > 13-fold). Therefore, GGPP and IL-18 are necessary in order to achieve a high γδ T-cell expansion and to prevent the toxic effect of zoledronate stimulation (**Fig. 21**).

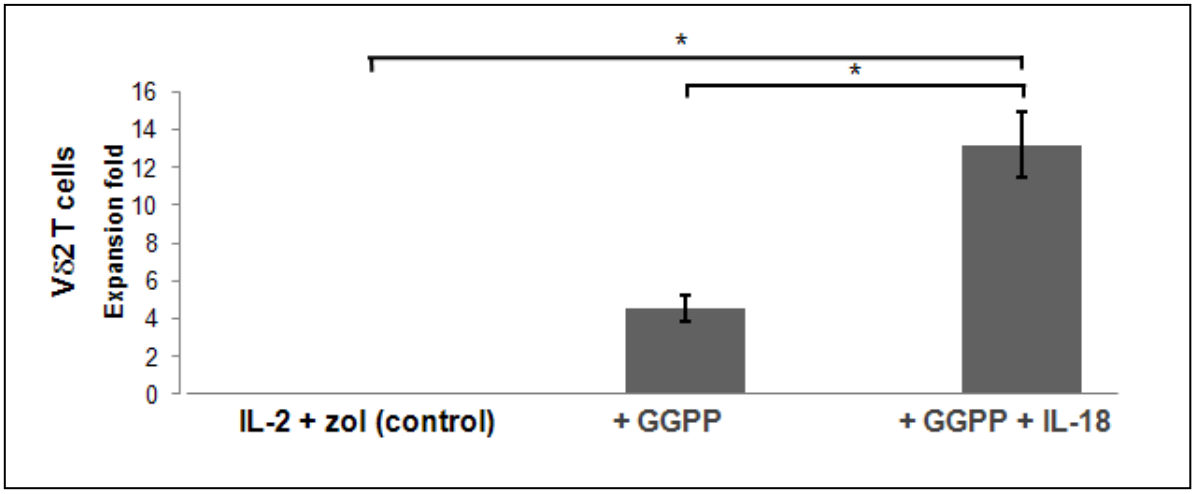

Figure 21: GGPP and IL-18 are required for high γδ T-cell-expansion in response to treatment with zoledronate plus IL-2. *Highly purified γδ T cells (10^5 per 96-well plate) were stimulated with zoledronate (10 µM) + IL-2 (100 U/ml) in combination with GGPP (10 µM) either alone or in combination with IL-18 (200 ng/ml). As a control γδ T cells were stimulated with IL-2 + zoledronate without other stimulation components. On day 10 the cells were stained for surface CD3 and TCR-Vδ2 and the γδ T-cell expansion was determined by flow cytometry. Finally, the cells were analysed by the BD FACSDiva™ software.*

*The total numbers of γδ T cells in the individual cell cultures were derived from absolute cell numbers considering γδ T-cell frequency and used to quantify γδ T-cell expansion. In Fig. 21 one experiment, which is representative of three independent experiments, is presented. The error bars are SD. * p < 0.05, zol: zoledronate.* ***Copyright 2013. The American Association of Immunologists, Inc.***

Previous studies have examined the relation between cell density and normal human T-cell expansion *in vitro*. Thereby, they have demonstrated that activated T cells undergo apoptosis at a low cell density of 1 x 10^4 cells and that PBMCs have to be seeded at high cell density (≥ 1 × 10^6/ml) for optimal T-cell activation (62). In our study we stimulated highly purified γδ T cells (**Fig. 22**) at low cell density (10^4 cells per well) with zoledronate plus IL-2 either alone or in combination with GGPP. Some cells were further stimulated with anti-IL-18 either alone or in combination with IL-1ß.

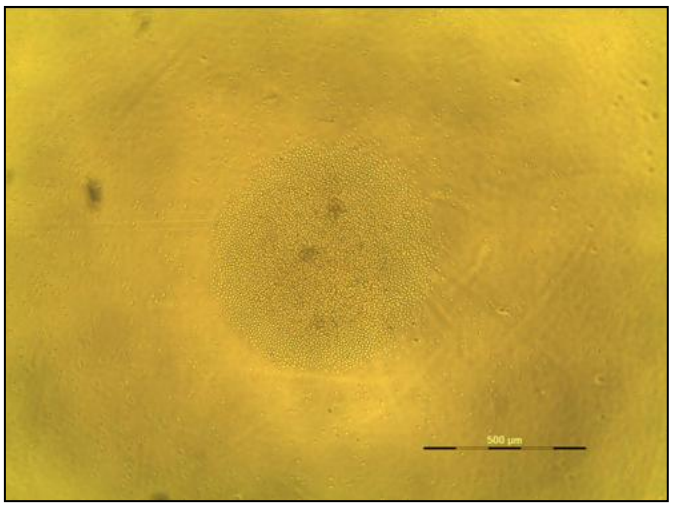

Figure 22: High resolution image of low γδ-T cell density on day 0. *Highly purified γδ T cells (10^4 cells per 96-well plate) were freshly seeded in 96-well plates. The cells were documented on day 0 with an Olympus CK2 microscope (magnification: 4×10) equipped with a ProgRes CT3 digital camera and ProgRes CapturePro 2.5 software (Jenoptik) The scale bar is 500 µm.* ***Copyright 2013. The American Association of Immunologists, Inc.***

At low cell density zoledronate killed more or less all γδ T cells due to toxic effects, whereas the addition of GGPP and IL-18 recovered γδ T cells also in critical cell density. No significant effect was observed with IL-1ß (**Fig. 23**).

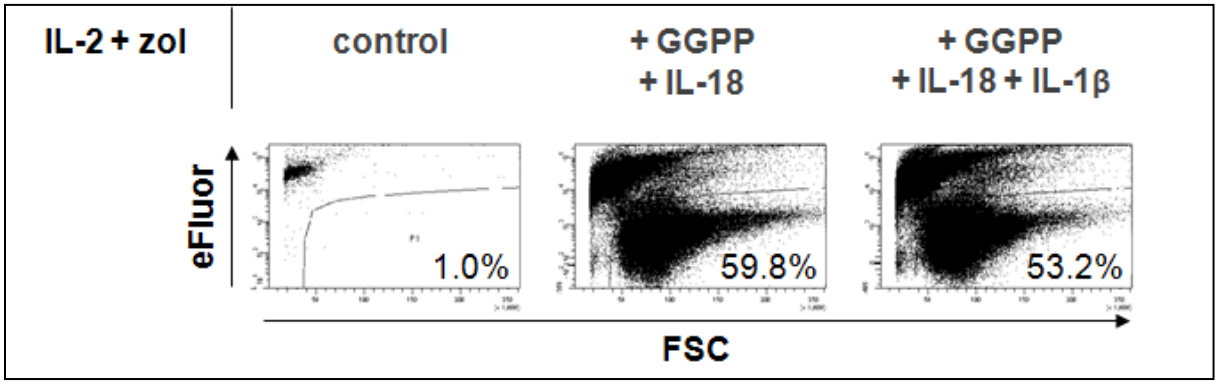

Figure 23: Low density γδ T cells were rescued by addition of GGPP plus IL-18. *γδ T cells were highly purified from PBMCs by negative selection. The cells were seeded at low cell density (10^4 cells per 96-well plate) and were treated with zoledronate (10 µM) + IL-2 (100 U/ml) either with GGPP (10 µM) and IL-18 (200 ng/ml) alone or combined with IL-1ß (5 ng/ml). The zoledronate toxicity was analysed on day 15 using eFluor 780 Fixable Viability Dye, which irreversibly labels dead cells. Finally, the cells were analysed by flow cytometry. The viable cells exclude eFluor and increase the forward scatter (FSC) during activation, zol: zoledronate.*

The low density γδ T cells were stained on day 15 for CD3 and TCR-Vδ2 to confirm γδ T-cell expansion. Our results demonstrated that supplementation of GGPP and IL-18 resulted in strong γδ T-cell expansion (~ 60 fold expansion), which could modestly be enhanced by the addition of IL-1ß [> 80 fold expansion, (**Fig. 24**)].

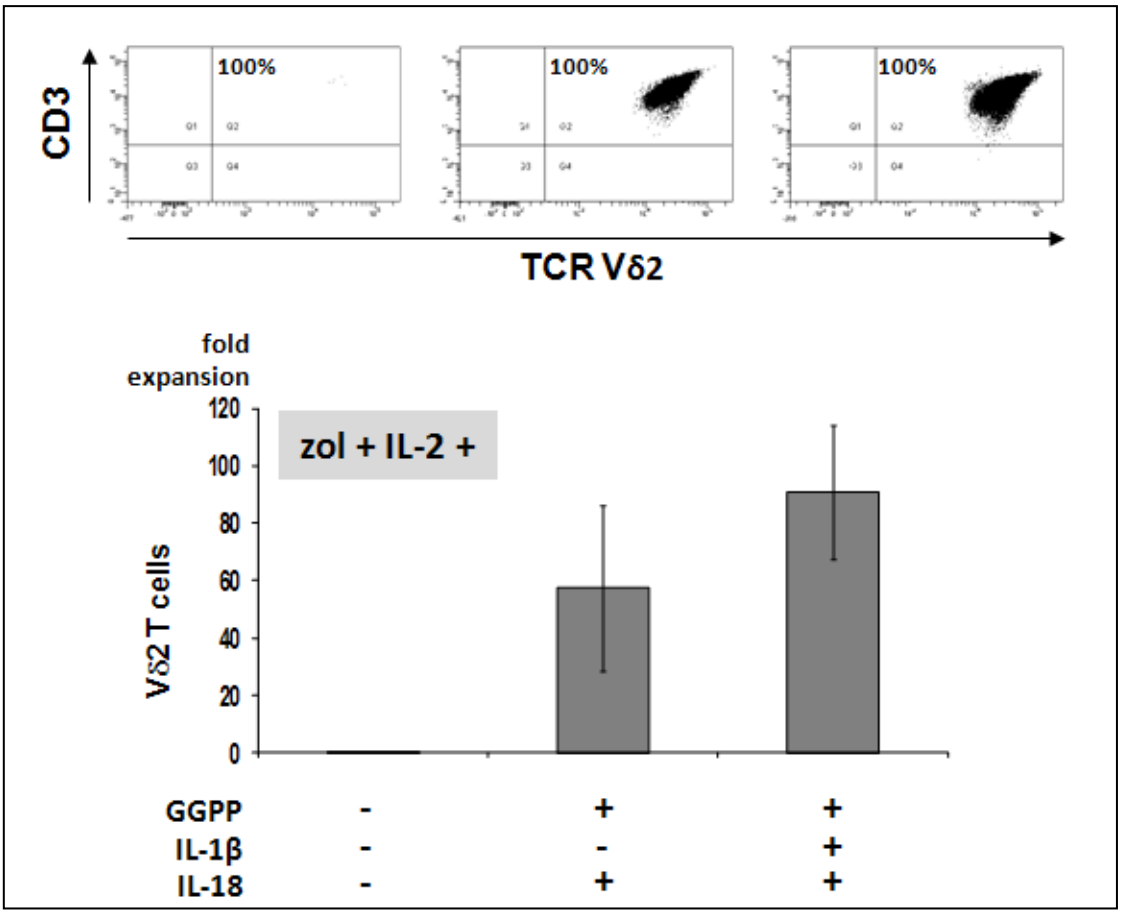

Figure 24: Addition of GGPP and IL-18 resulted in strong γδ T-cell expansion even at low cell density. *Highly purified γδ T cells (10^4 cells per 96-well plate) were stimulated with zoledronate (10 µM) + IL-2 (100 U/ml) in combination with GGPP (10 µM) and IL-18 (200 ng/ml) either alone or in combination with IL-1ß (5 ng/ml). As a control γδ T cells were stimulated with IL-2 + zoledronate without other stimulation components. On day 15 the cells were stained for surface CD3 and TCR-Vδ2. The γδ T-cell expansion was determined by flow cytometry and the cells were finally analysed by the BD FACSDiva™ software.*

*The total numbers of γδ T cells in the individual cell cultures were derived from absolute cell numbers considering γδ T-cell frequency and used to quantify γδ T-cell expansion. In Fig. 24 one experiment, which is representative of three independent experiments, is presented. The error bars are SD. * p < 0.05, zol: zoledronate.*

γδ T cells, even at low density, showed a time-dependent cell aggregation on day 3 and even higher aggregation on day 6. The costimulatory effect of IL-18 at critical cell density resulted in higher cell aggregation of γδ T cells and could be enhanced by supplementation with IL-1ß (**Fig. 25**).

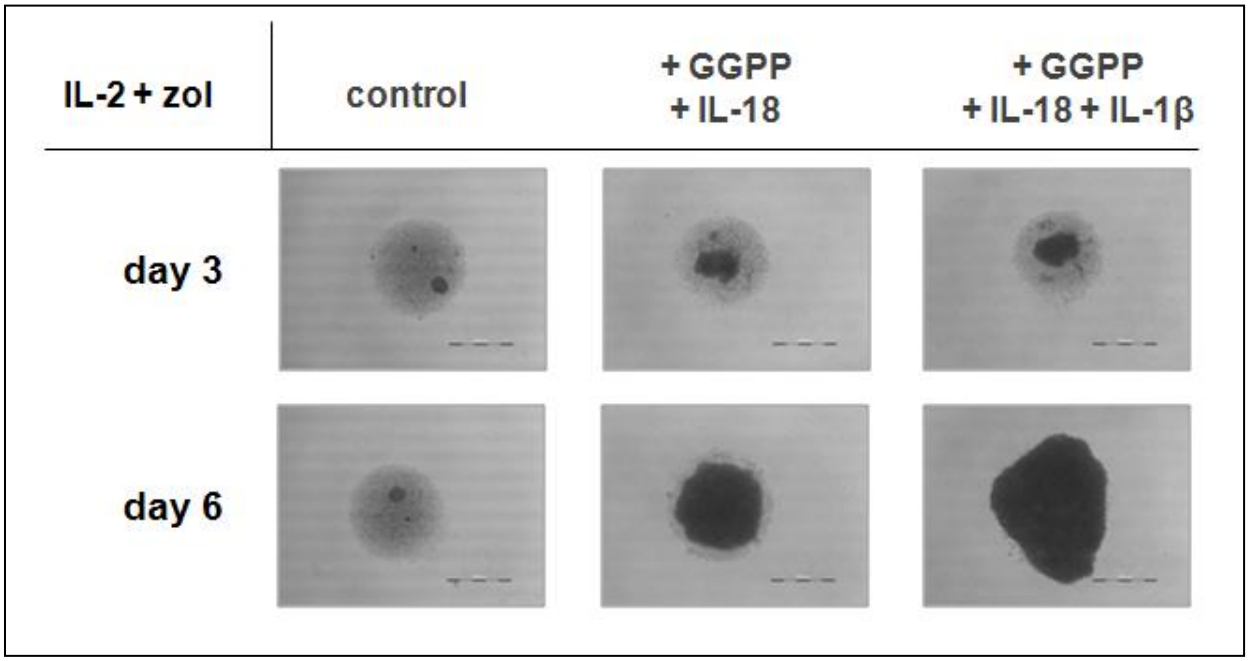

Figure 25: IL-18 costimulation resulted in higher cell aggregation of γδ T cells at low cell density. *Highly purified γδ T cells (10^4 cells per 96-well plate) were stimulated with zoledronate (10 µM) + IL-2 (100 U/ml) in combination with GGPP (10 µM) either alone or in combination with IL-18 (200 ng/ml). As a control γδ T cells were stimulated with IL-2 + zoledronate without other stimulation components.*

The different cell aggregation was documented on day 3 and day 6 with an Olympus CK2 microscope (magnification: 4×10) equipped with a ProgRes CT3 digital camera and ProgRes CapturePro 2.5 software (Jenoptik). The scale bar is 500 µm, zol: zoledronate.

4.6 Regulation of memory γδ T-cell differentiation

We have shown that addition of GGPP plus IL-18 resulted in higher γδ T-cell expansion by zoledronate plus IL-2 treated γδ T cells (**Fig. 24**). To examine the cell surface markers present on expanded γδ T cells, we performed experiments with highly purified γδ T cells. The cells were stimulated with IL-2 plus zoledronate in combination with either GGPP alone or with IL-18 costimulation, or with GGPP plus IL-18 plus IL-1ß for 14 days. Finally, the cells were stained for surface CD3, TCR-Vδ2, CD45RA and CD27. The γδ T-cell population on day 14 contained mainly T_{EM} cells. However, costimulation with IL-18 enhanced γδ T-cell expansion as well as differentiation of γδ T_{CM} cells. The final γδ T-cell population consisted of approximately equal numbers of T_{CM} and T_{EM} cells ($n = 4$, $p < 0.05$). The effect of IL-18 was not further enhanced by addition of IL-1ß (**Fig. 26**).

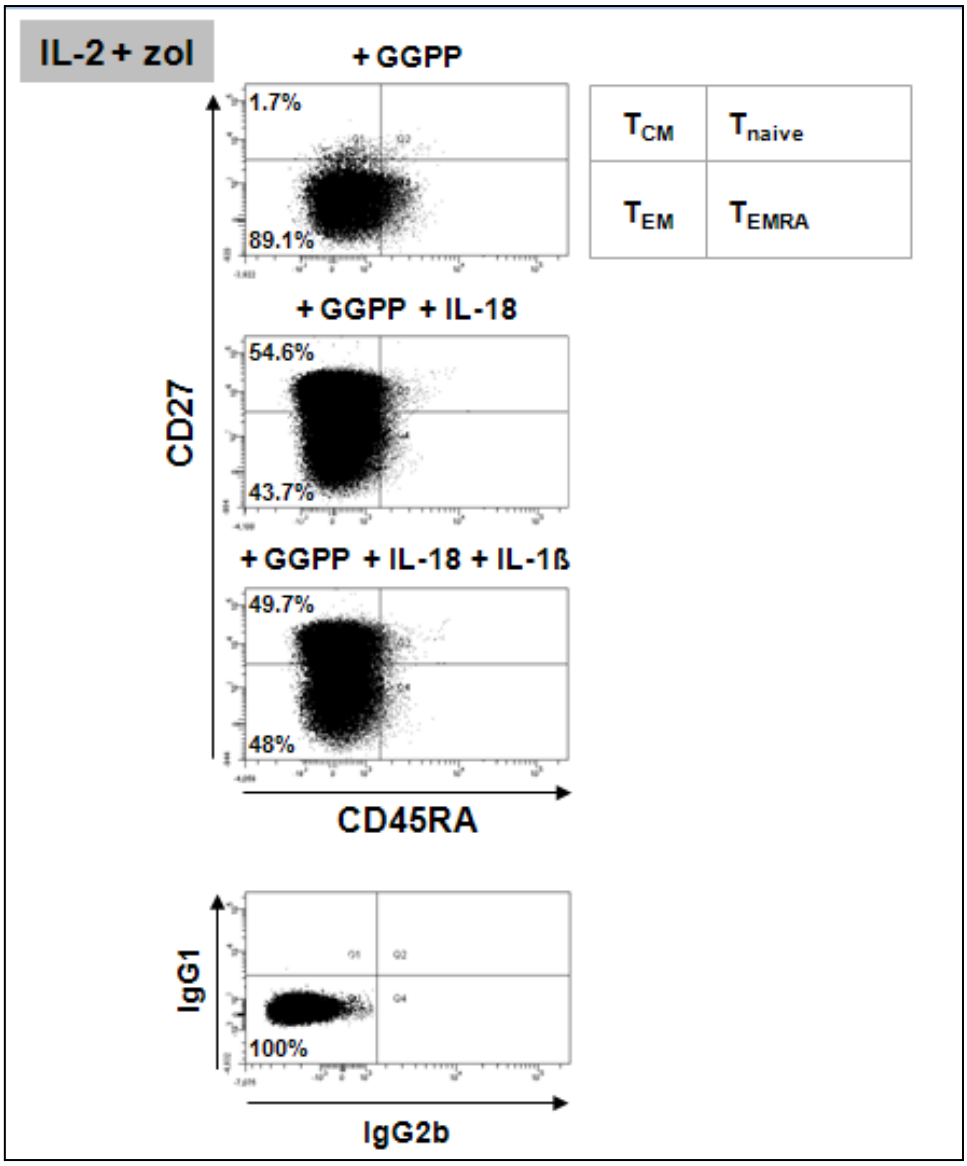

Figure 26: Phenotype analyses of highly purified γδ T cells treated with IL-2 plus zoledronate in combination with GGPP and IL-18. *Highly purified γδ T cells (10^4 cells per 96-well plate) were stimulated with zoledronate (10 µM) plus IL-2 (100 U/ml) in combination with GGPP (10 µM) either alone or in combination with IL-18 (200 ng/ml) or IL-2 plus zoledronate in combination with GGPP plus IL-18 and IL-1ß (5 ng/mL). On day 14 the cells were stained for surface CD3, TCR-Vδ2, CD45 RA and CD27 and the phenotypes γδ T cells were determined by flow cytometry and analysed using BD FACSDiva™ software.*

The phenotype of different cells: central memory T cells (T_{CM}, $CD45RA^{-}CD27^{+}$), effector memory T cells (T_{EM}, $CD45RA^{-}CD27^{-}$), terminally differentiated T cells (T_{EMRA}, $CD45^{+}CD27^{-}$), naïve T cells (T_{naive}, $CD45^{+}CD27^{+}$) (17), (26), γδ T cells ($CD3^{+}/Vδ2^{+}$). Bottom panel: For isotype control γδ T cells were treated with zoledronate plus IL-2 in combination of GGPP plus IL-18 and IL-1ß. The cells were stained for CD27 (IgG1) and CD45RA (IgG2b). In Fig. 26 one experiment, which is representative of four independent experiments, is presented, zol: zoledronate.

4.7 Analyses of cytokine response of highly purified γδ T cells

Recent studies have indicated that if γδ T cells were stimulated with IL-18, the cytokines TNF-α, GM-CSF and IFN-γ were produced at higher levels (47). The production of the effector cytokines IFN-γ and GM-CSF was examined. Highly purified γδ T cells were treated with zoledronate plus IL-2 in combination with GGPP either alone or with costimulation by IL-18 with or without IL-1ß. As a control γδ T cells were treated with zoledronate plus IL-2. The cells were stained on day 7 and the cytokine levels were determined in cell culture supernatants by CBA flex sets. In zoledronate plus IL-2-stimulated γδ T cells and in the presence of GGPP and IL-18, IFN-γ was upregulated. In the absence of IL-18, IFN-γ could not be detected. In addition we analysed the amount of the cytokine GM-CSF, which acts as an important cytokine for DC differentiation from monocytes and is therefore involved in adaptive αβ T-cell immune activation (49) (63). Interestingly, γδ T cells, which were incubated with IL-2 plus zoledronate with IL-18, showed high production levels of GM-CSF (**Fig. 27**). However, IL-17 was not detected in the culture supernatants (data not shown) even in combination with IL-1ß, which is supportive for differentiation into IL-17-producing human Vγ9Vδ2 T cells (64).

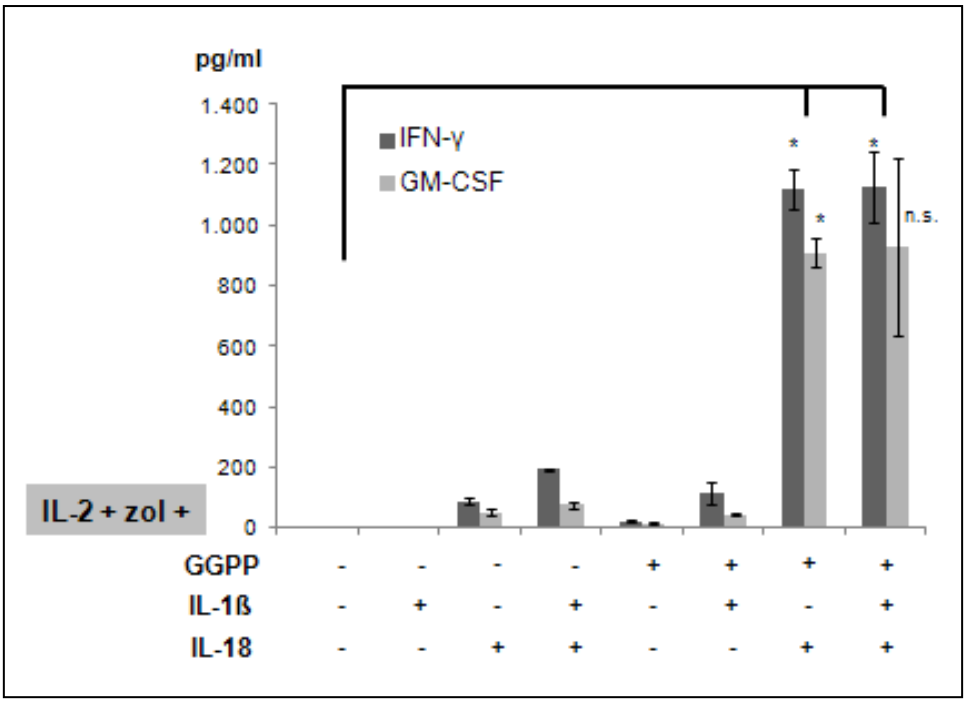

Figure 27: High levels of the cytokines GM-CSF and IFN-γ were determined in low density γδ T-cell cultures stimulated by zoledronate plus IL-2 in the presence of GGPP and IL-18. *Highly purified γδ T cells (10^4 cells per 96-well plate) were stimulated with zoledronate (10 µM) + IL-2 (100 U/ml) in combination with GGPP (10 µM) either alone or in combination with IL-18 (200 ng/ml), or GGPP plus IL-18 plus IL-1ß (5 ng/ml). As a control γδ T cells were stimulated with IL-2 + zoledronate without other stimulation components. The cytokines were analysed on day 7 in culture supernatants using CBA flex sets. In Fig. 27 one experiment, which is representative of three independent experiments, is shown. The error bars are SD. * p < 0.05; n.s.: not significant, zol: zoledronate.*

5. Discussion

The effect of zoledronate-induced inhibition of the FPP synthase in the mevalonate pathway seems to have two major effects: (i) the upstream accumulation of IPP and (ii) the deprivation of FPP and GGPP downstream of the mevalonate pathway (2). The upstream accumulation of IPP, which is recognised as an antigen by the Vγ9Vδ2 TCR on γδ T cells (18), (65), has immune stimulatory effects. This effect can be enhanced through the upregulation of the IL-2Rα on the surface of γδ T cells. Further, this results in a higher stimulatory effect of the cytokine IL-2, the T-cell growth factor (48).
The expression of IL-2Rα was induced by zoledronate plus IL-2 and mediated γδ T-cell proliferation. The depletion of monocytes, which are known to be one of the sources of both IL-18 and IL-1β (56), reduced the expression of the IL-2Rα. However, the addition of exogenous IL-18 could restore this effect and led to enhanced IL-2Rα expression. This finding led us to conclude that IL-18 is one of the major mediators of IL-2Rα upregulation.

However, the downstream depletion of the mevalonate intermediates FPP and GGPP showed also inhibitory effects. These two prenylpyrophosphates serve as substrates for prenylation on different heterotrimeric G-proteins, such as Ras, Rho and Rac (3). The inhibition of FPP (unpublished data) and especially GGPP via zoledronate treatment in combination with IL-2 resulted in an early cytokine response including IFN-γ, TNF-α, GM-CSF and IL-1ß. However, after depletion of monocytes, almost no or low amounts of the cytokines could be analysed. Moreover, zoledronate also mediated the upregulation of the chemokine CCL2 (MCP-1), which has not been shown before. It has recently been reported that the human and mouse γδ T cells, stimulated with CCL2/CCR2 migrate into tumour lesions, which had been observed by *in vivo* infiltration in murine tumour models (66). In addition the upregulation of these cytokines was enhanced in the presence of IL-18 costimulation.

Therefore it might be possible that zoledronate-related stress induction in combination with IL-18 costimulation upregulates CCL2 and therefore might orchestrate γδ T-cell migration to stressed tissues such as tumours. Additionally, the inhibitory effect of the downstream depletion of pyrophosphates resulted in a delayed γδ T-cell expansion, which was further enlarged if the monocytes were depleted.

Monocytes are generally suggested to be involved in zoledronate-mediated Vγ9Vδ2 T-cell activation, as they serve as a source of IPP/DMAPP (67) and are also known to be a source of costimulatory cytokines like IL-18 and IL-1β (56). Roelofs *et al.* hypothesised that N-BPs are internalised by monocytes via their high endocytic activity. The internalisation further leads to accumulation of the antigen IPP and its stereoisomer DMAPP in order to activate Vγ9Vδ2 T cells. In this study they used quantitative mass spectrometry to analyse human PBMC cultures treated with zoledronate for 2 hours. Whereas no IPP/DMAPP accumulation was detected in untreated cells, zoledronate triggered the accumulation of IPP/DMAPP in monocytes. They further demonstrated that zoledronate-treated monocytes enhanced the IFN-γ release and additionally increased the Vδ2 T-cell number (67).
Our results demonstrated that monocytes rather are a source of the cytokine IL-18, after zoledronate stimulation resulting in caspase-1 activation (2), (43). The depletion of monocytes resulted also in a decrease production of cytokines. Moreover, zoledronate plus IL-2 mediated cytokine response was reduced in presence with an IL-18 neutralising antibody.
Treatments with zoledronate plus IL-2 in combination with IL-18 neutralising antibody reduced the production of all analysed cytokines. Depletion of monocytes, which serve as a source of IL-18 (56), led to reduced expression of the IL-2Rα on the surface of γδ T cells. The importance of IL-18 was confirmed by the upregulation of IL-2Rα through addition of exogenous IL-18 in absence of any accessory cells.

The delayed response of zoledronate-mediated γδ T-cell expansion due to downstream depletion of the prenyl pyrophosphates was skipped by addition of GGPP (10 µM). Supplementation with GGPP also enhanced γδ T-cell expansion, which was further amplified by costimulation with IL-18. These findings lead us to examine the role of accessory cells including monocytes, DCs, B cells and activated T cells and $CD56^+$ cells. The fact that IL-18 stimulated γδ T cells also after depletion of all accessory cells indicated that IL-18 directly stimulates γδ T cells. In cultures with purified γδ T cells zoledronate was particularly toxic due to zoledronate-mediated inhibition of FPP synthase, which leads to downstream depletion of the prenyl pyrophosphates (2), (3). However, addition of the mevalonate intermediate GGPP could prevent this toxic effect. Treatment with GGPP and IL-18 costimulation led to a very strong γδ T-cell expansion, which could be also achieved at such a low cell density (10^4 cells per 96 well). Usually, T cells stimulated at such a low cell density undergo apoptosis due to oxidative stress (62). Therefore, our findings might be very useful to optimise the γδ T-cell expansion even starting from low cell densities. Hence, the γδ T-cell expansion can be improved from small blood samples or tissue samples in order to use them for immunotherapy in cancer patients.

Previous studies have postulated that monocytes are the only cells, which are able to produce IPP in response to zoledronate treatment (67). Our results demonstrated that γδ T cells could be expanded even in absence of any accessory cells including monocytes. Brandes *et al.* have demonstrated that γδ T cells can aquire accessory cell features after activation with the specific antigen IPP (27). The same group demonstrated that γδ T cells aquire also endocytic activity, which is important to take up zoledronate (68). Moreover, the phosphoantigen-dependent activation of γδ T cells and their accessory potential can be enhanced by CD70-CD27 costimulation, which positively influences proliferation, survival and cytokine production (53), (54).

The $CD56^{bright}CD11c^{+}$ NK cells, another type of accessory cells, are involved in the IL-18 mediating effect of zoledronate-induced γδ T-cell expansion (52). Although, all accessory cells were depleted, including $CD56^{+}$ cells, we observed that IL-18 also showed stimulating effects on highly purified γδ T cells indicating that IL-18 directly stimulates γδ T cells. In addition, the diminished expansion in the presence of $CD56^{+}$ cells, which may be due to IL-18-mediated activation of NK-cell cytotoxicity, was in contrast with the study of Tsuda *et al.* They have suggested that $CD56^{+}$ cell depletion may impair γδ T-cell expansion by eliminating $CD56^{bright}CD11c^{+}$ NK cells as accessory cells (52).

Our findings also demonstrated that IL-18 upregulated CD56 expression on the surface of γδ T cells, which might have a higher resistance to Fas-ligand-mediated apoptosis as well as chemically induced-apoptosis and to be more cytotoxic against tumour cells (61).
Furthermore, IL-18 has been identified to be a promising target for cancer therapy. In the study of Yao *et al*. the observed that IL-18 might be involved in doxorubicin resistance of MCF-7 breast cancer cells. The findings that in presence of IL-18 the survival rate of MCF-7 was increased after doxorubicin treatment (69) are similar to our results that IL-18 may have important effects to impair the zoledronate toxicity in order to improve the γδ T-cell proliferation, also within highly purified γδ T cells.

We have also observed that IL-18 influences the differentiation of highly purified γδ T cells during zoledronate treatment. The γδ T-cell population mainly consisted of T_{EM} cells after the stimulation with zoledronate plus IL-2 and costimulated with GGPP in the absence of IL-18. However, in the presence of IL-18 the final γδ T-cell population consisted of approximately equal numbers of T_{CM} and T_{EM} cells.

The costimulation with IL-18 results in both cell types, in cells with immediate effector function and in cells with memory phenotypes for long-term protection function. Additionally, T_{CM} cells may have higher ability than T_{EM} cells to persist *in vivo* and may be able to mediate higher protection because of their strong proliferative potential, like reported for $\alpha\beta$ T_{CM} cells (70). This potential might be attributed to the expression of CD27 receptor, which improves proliferation upon costimulation with its ligand CD70 (53). Therefore IL-18 not only stimulated γδ T cells but also positively influenced the γδ T-cell differentiation. This might be useful to establish the important requirements in order to open new perspectives for modulating clinical cancer immunotherapy.

Whereas, γδ T cells were seen as the important source of IL-17 under certain circumstances (71), we could detect this proinflammatory cytokine neither in PBMCs nor in purified γδ T cells. It has been reported that IL-1β and IL-18 promote IL-17 production in mice (72). In our study of human blood cells IL-17 was not possible to detect, even in presence of these two cytokines. Recent studies have indicated that human naive Vγ9Vδ2 T cells could differentiate toward IL-17 producing cells by TCR triggering and stimulation with different cytokines, namely IL-1ß, IL-6, TGF-ß and IL-23. Accordingly, $IL17^+$ Vγ9Vδ2 T cells exhibited a T_{EMRA} phenotype as they expressed $CD45RA^+CD27^-$ surface subsets (64). Consequently, our results showed that stimulation of highly purified γδ T cells with IL-18 did not result in IL-17 production as well as no expression of T_{EMRA} phenotypes. At the moment it is unclear if the lack of T_{EMRA} γδ T cells (19), (29) is based on missing differentiation factors to enable these cells or is caused through the early death due to the developed effector functions (cytolysis or cytokine production).

In summary, we determined critical aspects of induction of γδ T-cell proliferation as well as the capacity to recognise antigens in order to sense infections or other forms of stress resulting in clonal γδ T-cell expansion (23). Through inhibition of the FPP synthase in the mevalonate pathway and the downstream depletion of the prenyl pyrophosphates, zoledronate-induced cell stress resulted in inflammasome activation. Hence, the IL-1 converting enzyme caspase-1 generates the active form of IL-18 (2), (43). Inflammasome activation through zoledronate also mediated the upregulation of the chemokine CCL2 (MCP-1), which might direct γδ T-cell migration to stressed tissues such as tumours (66).

According to our observations IL-18 enables γδ T-cell expansion from low cell density (10^4 cells) as well as the production of the cytokines TNF-α, GM-CSF and IFN-γ. Beyond that, GM-CSF may enable the DC differentiation from monocytes and is therefore an important factor for adaptive $\alpha\beta$ T-cell immune activation (49), (63).

6. Abstract

Zoledronate inhibits farnesyl pyrophosphate (FPP) synthase, a key enzyme in the mevalonate pathway, which is often upregulated in malignant cells and therefore serves as an important therapeutic target. On the one hand inhibiting the FPP synthase results in upstream accumulation of the antigen IPP and on the other hand it results in downstream depletion of the isoprenoid pyrophosphates FPP and geranyl geranyl pyrophosphate (GGPP), which are required for protein prenylation. Vγ9Vδ2 T cells sense infections or other forms of stress in an innate-like way. They expand due to the accumulation of the potent antigen IPP, which is recognised by the Vγ9Vδ2 T-cell receptor (TCR). Previous studies have indicated that γδ T cells require accessory cells for optimal expansion. Monocytes are able to produce IPP and therefore are important for γδ T-cell expansion. In addition $CD56^{bright}CD11c^{+}$ NK cells, which are involved to mediate the effect of IL-18 on γδ T-cell expansion, are important accessory cells involved in γδ T-cell expansion. In our study we demonstrate that the downstream depletion of GGPP results in caspase-1-mediated release of the active form of IL-18, which further induces the upregulation of IL-2 receptor α chain (IL-2Rα, CD25). The upregulation of IL-2Rα is followed by an early cytokine response, which included the production of the γδ T-cell chemokine (C-C motif) ligand 2 (CCL2). We observed a delay in zoledronate-induced γδ T-cell proliferation, which could be skipped by addition of GGPP. Supplementation of GGPP prevented acute zoledronate toxicity. Furthermore our experiments showed that IL-18 positively influenced γδ T-cell differentiation of central memory T cells (T_{CM}). Additionally, IL-18 induced proliferation of highly purified γδ T cells, even when the starting frequency was very low (10^4 γδ T cells). In highly purified γδ T cells, the γδ T-cell expansion was achieved through supplementation of exogenous IL-18. Therefore in our experiments we demonstrated that IL-18 directly costimulates γδ T cells without the requirement of accessory cells. Our study contributes to a better understanding of the γδ T-cell activation. Such robust γδ T cells may be harnessed for clinical immunotherapy of cancer and infectious diseases.

7. Zusammenfassung

Zoledronat hemmt die Farnesyl Pyrophosphat (FPP) Synthase, ein Schlüsselenzym im Mevalonat-Stoffwechselweg. Dieser Stoffwechsel ist in Krebszellen sehr oft hochreguliert und dient deshalb als therapeutischer Angriffspunkt. Die Hemmung der FPP Synthase hat zwei Effekte, die Anhäufung von Isopentenyl Pyrophosphat (IPP) und die Depletion von FPP und Geranylgeranyl Pyrophosphat (GGPP), welche als biochemisch aktivierte Isoprenoide bei der Proteinprenylierung eine wichtige Rolle spielen. Die Vγ9Vδ2 T Zellen reagieren auf Infektionen und andere Formen von Stress als Zellen des angeborenen Immunsystems. Häuft sich das potente Antigen IPP an, wird es von den Vγ9Vδ2 T Zellen mittels ihres T-Zell Rezeptors erkannt und es kommt zu einer verstärkten Aktivierung der Zellen. Frühere Studien belegen, dass nach Zugabe von Zoledronat die Monozyten eine wichtige Quelle für IPP darstellen. Darüber hinaus, dienen $CD56^+$ NK Zellen als wichtige akzessorische Zellen im Zusammenhang mit der γδ T-Zell Aktivierung. Es wurde gezeigt, dass $CD56^+$ NK Zellen durch IL-18, das von Monozyten freigesetzt wird, aktiviert werden und daraufhin die γδ T Zellen kostimulieren. In unserer Studie zeigen wir, dass die Depletion von GGPP zur Caspase-1 vermittelten Freisetzung der aktiven Form von IL-18 führt. Die Freisetzung von IL-18 führte zur einen höheren Expression des IL-2 Rezeptors (IL-2Rα, CD25). Darüber hinaus kommt es nach Zugabe von Zoledronat in der Kombination mit IL-2 und GGPP zu einer frühen Zytokinproduktion, inklusive des γδ T-Zell Chemokine (C-C motif) Liganden 2 (CCL2). Die von Zoledronat vermittelte γδ T-Zell Aktivierung war verzögert, konnte aber durch Zugabe von GGPP beschleunigt werden, da GGPP die Toxizität von Zoledronat aufhebt. IL-18 hatte einen Einfluss auf die γδ T-Zell Differenzierung und führte zu einer höheren Expression von „central memory T cells (T_{CM})“. Durch exogen verabreichtes IL-18 konnte eine γδ T-Zell-Expansion von reinen γδ T Zellen erreicht werden, sogar bei einer geringen Startpopulation (10^4 γδ T Zellen). Deshalb wirkt IL-18 offensichtlich direkt, ohne dass eine IL-18 vermittelte Wirkung von $CD56^+$ NK Zellen benötigt wird. Unsere Erkenntnisse führen zu einem besseren Verständnis der γδ T-Zell Aktivierung. Diese robusten γδ T Zellen können dann in medizinisch angewandten Immuntherapien gegen Krebs und Infektionskrankheiten genutzt werden.

8. References

1. **Goldstein JL, Brown Ms.** Regulation of the mevalonate pathway. *Nature.* 1990, 343:425-30.

2. **Thurnher M, Nussbaumer O, Gruenbacher G.** Novel aspects of mevalonate pathway inhibitors as antitumor agents. *Clin Cancer Res.* 2012, 18(13):3524-31.

3. **Casey PJ, Seabra MC.** Protein prenyltransferase. *J Biol Chem.* 1996, 271(10):5289-92.

4. **Freed-Pastor WA, Mizuno H, Zhao X, Langerød A, Moon SH, Rodriguez-Barrueco R, Barsotti A, Chicas A, Li W, Polotskaia A, Bissell MJ, Osborne TF, Tian B, Lowe SW, Silva JM, Børresen-Dale AL, Levine AJ, Bargonetti J, Prives C.** Mutant p53 disrupts mammary tissue architecture via the mevalonate pathway. *Cell.* 2012, 148(1-2):244-58.

5. **Thurnher M, Gruenbacher G, Nussbaumer O.** Regulation of mevalonate metabolism in cancer and immune cells. *Biochim Biophys Acta.* 2013, 1831(6):1009-15.

6. **Russel, RG.** Bisphosphonates: the first 40 years. *Bone.* 2011, 49(1):2-19.

7. **Berenson JR, Hillner BE, Kyle RA, Anderson K, Lipton A, Yee GC, Biermann JS.** American Society of Clinical Oncology Bisphosphonates Expert Panel. American Society of Clinical Oncology clinical practice guidelines: the role of bisphosphonates in multiple myeloma. *Clin Oncol.* 2002, 20:3719-36.

8. **Mitrofan LM, Pelkonen J, Mönkkönen J.** The level of ATP analog and isopentenyl pyrophosphate correlates with zoledronic acid-induced apoptosis in cancer cells in vitro. *Bone.* 2009, 45:1153-60.

9. **Jahnke W, Rondeau JM, Cotesta S, Marzinzik A, Pellé X, Geiser M, Strauss A,Götte M, Bitsch F, Hemmig R, Henry C, Lehmann S, Glickman JF, Roddy TP, Stout SJ, Green JR.** Allosteric non-bisphosphonate FPPS inhibitors identified by fragment-based discovery. *Nat Chem Biol.* 2010, 6(9):660-6.

10. **Morita CT, Jin C, Sarikonda G, Wang H.** Nonpeptide antigens, presentation mechanisms, and immunological memory of human Vgamma2Vdelta2 T cells: discriminating friend from foe through the recognition of prenyl pyrophosphate antigens. *Immunol Rev.* 2007, 215:59-76.

11. **Riebeling C, Forsea AM, Raisova M, Orfanos CE, Geilen CC.** The bisphosphonate pamidronate induces apoptosis in human melanoma cells in vitro. *Br J Cancer.* 2002, 87(3):366-71.

12. **Castella B, Vitale C, Coscia M, Massaia M.** Vγ9Vδ2 T cell-based immunotherapy in hematological malignancies: from bench to bedside. *Cell Mol Life Sci.* 2011, 68 (14): 2419-32.

13. **Pozzi S, Raje N.** The role of bisphosphonates in multiple myeloma: mechanisms, side effects, and the future. *Oncologist.* 2011, 16:651-62.

14. **Gnant M.** Can oral bisphosphonates really reduce the risk of breast cancer in healthy women? *J Clin Oncol.* 2010, 28:3548-51.

15. **Michaelson MD, Smith MR.** Bisphosphonates for treatment and prevention of bone metastases. *J Clin Oncol.* 2005, 23:8219-24.

16. **Ramaswamy B, Shapiro CL.** Bisphosphonates in the prevention and treatment of bone metastases. *Oncology (Williston Park).* 2003, 17(9):1261-70.

17. **van der Burgh R, Ter Haar NM, Boes ML, Frenkel J.** Mevalonate kinase deficiency, a metabolic autoinflammatory disease. *Clin Immunol.* 2012, doi:pii: S1521-6616(12)00236-7.

18. **Tanaka Y, Morita CT, Tanaka Y, Nieves E, Brenner MB, Bloom BR.** Natural and synthetic non-peptide antigens recognized by human gamma delta T cells. *Nature.* 1995, 375(6527):155-8.

19. **Kabelitz D, He W.** The multifunctionality of human Vg9Vd2 gd T cells: clonal plasticity or distinct subsets? *Scand J Immunol.* 2012, 76(3):213-22.

20. **Lanier LL.** Shades of grey--the blurring view of innate and adaptive immunity. *Nat Rev Immunol.* 2013, 13(2):73-4.

21. **Wang JH, Reinherz EL.** The structural basis of αβ T-lineage immune recognition:TCR docking topologies, mechanotransduction, and co-receptor function. *Immunol Rev.* 2012, 250(1):102-19.

22. **Hannani D, Ma Y, Yamazaki T, Déchanet-Merville J, Kroemer G, Zitvogel L.** Harnessing gd T cells in anticancer immunotherapy. *Trends Immunol.* 2012, 33 (5) : 199-206.

23. **Vantourout P, Hayday A.** Six-of-the-best: unique contributions of gd T cells to immunology. *Nat Rev Immunol.* 2013, 13(2):88-100.

24. **Hayday AC.** [gamma][delta] cells: a right time and a right place for a conserved third way of protection. *Annu Rev Immunol.* 2000, 18:975-1026.

25. **Holtmeier W, Pfänder M, Hennemann A, Zollner TM, Kaufmann R, Caspary WF.** The TCR-delta repertoire in normal human skin is restricted and distinct from the TCR-delta repertoire in the peripheral blood. *J Invest Dermatol.* 2001, 116(2) :275-80.

26. **Jutila MA, Holderness J, Graff JC, Hedges JF.** Antigen-independent priming: a transitional response of bovine gammadelta T-cells to infection. *Anim Health Res Rev.* 2008, 9(1):47-57.

27. **Brandes M, Willimann K, Moser B.** Professional antigen-presentation function by human gammadelta T Cells. *Science.* 2005, 309(5732) : 264-8.

28. **Saito T, Hochstenbach F, Marusic-Galesic S, Kruisbeek AM, Brenner M, Germain RN.** Surface expression of only gamma delta and/or alpha beta T cells receptor heterodimers by cells with four (alpha, beta, gamma, delta) functional receptor chains. *J Exp Med.* 1988, 168 (3) : 1003-20.

29. **Dieli F, Vermijlen D, Fulfaro F, Caccamo N, Meraviglia S, Cicero G, Roberts A,Buccheri S, D'Asaro M, Gebbia N, Salerno A, Eberl M, Hayday AC.** Targeting human{gamma}delta} T cells with zoledronate and interleukin-2 for immunotherapy of hormone-refractory prostate cancer. *Cancer Res.* 2007, 67(15):7450-7.

30. **Holderness J, Hedges JF, Ramstead A, Jutila MA.** Comparative Biology of γδ T Cell Function in Humans, Mice, and Domestic Animals. *Annu. Rev. Anim. Biosci.* 2013, 1:99-124.

31. **Kunzmann V, Bauer E, Wilhelm M.** Gamma/delta T-cell stimulation by pamidronate. *N Engl J Med.* 1999, 340(9):737-8.

32. **Hintz M, Reichenberg A, Altincicek B, Bahr U, Gschwind RM, Kollas AK, Beck E, Wiesner J, Eberl M, Jomaa H.** Identification of (E)-4-hydroxy-3-methyl-but-2-enyl pyrophosphate as a major activator for human gammadelta T cells in Escherichia coli. *FEBS Lett.* 2001, 509(2) :317-22.

33. **Eberl M, Moser B.** Monocytes and gammadelta T cells: close encounters in microbial infection. *Trends Immunol.* 2009, 30(12):562-8.

34. **Jiang Y, Guo Y, Xi X, Cui L, He W.** Flanking V and J sequences of complementary determining region 3 of T cell receptor (TCR) d1 (CDR3d1) determine the structure and function of TCRg4d1. *J Biol Chem.* 2011, 286(29) : 25611-9.

35. **Braza MS, Klein B.** Anti-tumour immunotherapy with Vγ9Vδ2 T lymphocytes: from the bench to the bedside. *Br J Haematol.* 2013, 160(2) : 123-32.

36. **Gomes AQ, Martins DS, Silva-Santos B.** Targeting γδ T lymphocytes for cancer immunotherapy: from novel mechanistic insight to clinical application. *15. Gomes AQ, Martins DS, Silva-Santos B. Targeting γδ T lymphocytes for cancer immunoCancer Res.* 2010, 70: 10024-7.

37. **Dieli F, Gebbia N, Poccia F, Caccamo N, Montesano C, Fulfaro F, Arcara C, Valerio MR, Meraviglia S, Di Sano C, Sireci G, Salerno A.** Induction of gammadelta T-lymphocyte effector functions by bisphosphonate zoledronic acid in cancer patients in vivo. *Blood.* 2003, 102(6) : 2310-1.

38. **Meraviglia S, Eberl M, Vermijlen D, Todaro M, Buccheri S, Cicero G, La Mendola C, Guggino G, D'Asaro M, Orlando V, Scarpa F, Roberts A, Caccamo N, Stassi G,Dieli F, Hayday AC.** In vivo manipulation of Vgamma9Vdelta2 T cells with zoledronate and low-dose interleukin-2 for immunotherapy of advanced breast cancer patients. *Clin Exp Immunol.* 2010, 161(2):290-7.

39. **Argentati K, Re F, Serresi S, Tucci MG, Bartozzi B, Bernardini G, Provinciali M.** Reduced number and impaired function of circulating gamma delta T cells in patients with cutaneous primary melanoma. *J Invest Dermatol.* 2003, 120(5):829-34.

40. **Noguchi A, Kaneko T, Kamigaki T, Fujimoto K, Ozawa M, Saito M, Ariyoshi N,Goto S.** Zoledronate-activated Vγ9γδ T cell-based immunotherapy is feasible and restores the impairment of γδ T cells in patients with solid tumors. *Cytotherapy.* 2011, 13(1):92-7.

41. **Kunzmann V, Bauer E, Feurle J, Weissinger F, Tony HP, Wilhelm M.** Stimulationof gammadelta T cells by aminobisphosphonates and induction of antiplasma cell activity in multiple myeloma. *Blood.* 2000, 96(2) :384-92.

42. **Gober HJ, Kistowska M, Angman L, Jenö P, Mori L, De Libero G.** Human T cell receptor gammadelta cells recognize endogenous mevalonate metabolites in tumor cells. *J Exp Med.* 2003, 197(2) : 163-8.

43. **Pontillo A, Paoluzzi E, Crovella S.** The inhibition of mevalonate pathway induces upregulation of NALP3 expression: new insight in the pathogenesis of mevalonate kinase deficiency. *Eur J Hum Genet.* 2010, 18(7) :844-7.

44. **Sims JE, Smith DE.** The IL-1 family: regulators of immunity. *Nat Rev Immunol.* 2010, 10(2): 89-102.

45. **Nakanishi K, Yoshimoto T, Tsutsui H, Okamura H.** Interleukin-18 regulates both Th1 and Th2 responses. *Annu Rev Immunol.* 2001, 19:423-74.

46. **Nussbaumer O, Gruenbacher G, Gander H, Thurnher M.** DC-like cell-dependent activation of human natural killer cells by the bisphosphonate zoledronic acid is regulated by gammadelta T lymphocytes. *Blood.* 2011, 118: 2743-2751.

47. **Li W, Kubo S, Okuda A, Yamamoto H, Ueda H, Tanaka T, Nakamura H, Yamanishi H, Terada N, Okamura H.** Effect of IL-18 on expansion of gammadelta T cells stimulated by zoledronate and IL-2. *J Immunother.* 2010, 33(3):287-96.

48. **Liao W, Lin JX, Leonard WJ.** IL-2 family cytokines: new insights into the complex roles of IL-2 as a broad regulator of T helper cell differentiation. *Curr Opin Immunol.* 2011, 23(5):598-604.

49. **van de Laar L, Coffer PJ, Woltman AM.** Regulation of dendritic cell development by GM-CSF: molecular control and implications for immune homeostasis and therapy. *Blood.* 2012, 119(15):3383-93.

50. **Song C, Luo L, Lei Z, Li B, Liang Z, Liu G, Li D, Zhang G, Huang B, Feng ZH.** IL-17-producing alveolar macrophages mediate allergic lung inflammation related to asthma. *J Immunol.* 2008, 181(9):6117-24.

51. **Ferretti S, Bonneau O, Dubois GR, Jones CE, Trifilieff A.** IL-17, produced by lymphocytes and neutrophils, is necessary for lipopolysaccharide-induced airway neutrophilia: IL-15 as a possible trigger. *J Immunol.* 2003, 170(4):2106-12.

52. **Tsuda J, Li W, Yamanishi H, Yamamoto H, Okuda A, Kubo S, Ma Z, Terada N,Tanaka Y, Okamura H.** Involvement of CD56brightCD11c+ cells in IL-18-mediated expansion of human γδ T cells. *J Immunol.* 2011, 186(4):2003-12.

53. **DeBarros A, Chaves-Ferreira M, d'Orey F, Ribot JC, Silva-Santos B.** CD70-CD27 interactions provide survival and proliferative signals that regulate T cell receptor-driven activation of human γδ peripheral blood lymphocytes. *Eur J Immunol.* 2011, 41(1):195-201.

54. **Ribot JC, debarros A, Silva-Santos B.** Ribot JC, debarros A, Silva-Santos B. Searching for "signal 2": costimulation requirements of γδ T cells. *Cell Mol Life Sci.* 2011, 68(14):2345-55.

55. **Gruenbacher G, Gander H, Nussbaumer O, Nussbaumer W, Rahm A, Thurnher M.** IL-2 costimulation enables statin-mediated activation of human NK cells, preferentially through a mechanism involving CD56+ dendritic cells. *Cancer Res.* 2010, 70(23):9611-20.

56. **Okamura H, Tsutsi H, Komatsu T, Yutsudo M, Hakura A, Tanimoto T, Torigoe K,Okura T, Nukada Y, Hattori K, et al.** Cloning of a new cytokine that induces IFN-gamma production by T cells. *Nature.* 1995, 378(6552):88-91.

57. **Fantuzzi G, Dinarello CA.** Fantuzzi G, Dinarello CA. Interleukin-18 and interleukin-1 beta: two cytokine substrates for ICE (caspase-1). *J Clin Immunol.* 1999, 19(1) :1-11.

58. **Thornberry NA, Peterson EP, Zhao JJ, Howard AD, Griffin PR, Chapman KT.** Inactivation of interleukin-1 beta converting enzyme by peptide (acyloxy)methyl ketones. *Biochemistry.* 1994, 33(13):3934-40.

59. **Carr MW, Roth SJ, Luther E, Rose SS, Springer TA.** Monocyte chemoattractant protein 1 acts as a T-lymphocyte chemoattractant. *Proc Natl Acad Sci U S A.* 1994, 91(9):3652-6.

60. **Matsushima K, Larsen CG, DuBois GC, Oppenheim JJ.** Purification and characterization of a novel monocyte chemotactic and activating factor produced by a human myelomonocytic cell line. *J Exp Med.* 1989, 169(4):1485-90.

61. **Alexander AA, Maniar A, Cummings JS, Hebbeler AM, Schulze DH, Gastman BR, Pauza CD, Strome SE, Chapoval AI.** Isopentenyl pyrophosphate-activated CD56+ {gamma}{delta} T lymphocytes display potent antitumor activity toward human squamous cell carcinoma. *Clin Cancer Res.* 2008, 14(13):4232-40.

62. **Ma Q, Wang Y, Lo AS, Gomes EM, Junghans RP.** Cell density plays a critical role in ex vivo expansion of T cells for adoptive immunotherapy. *J Biomed Biotechnol.* 2010, 2010:386545.

63. **Steinman, RM.** Decisions about dendritic cells: past, present, and future. *Annu Rev Immunol.* 2012, 30:1-22.

64. **Caccamo N, La Mendola C, Orlando V, Meraviglia S, Todaro M, Stassi G, Sireci G, Fournié JJ, Dieli F.** Differentiation, phenotype, and function of interleukin-17-producing human Vγ9Vδ2 T cells. *Blood.* 2011, 118(1):129-38.

65. **Gruenbacher G, Gander H, Rahm A, Nussbaumer W, Romani N, Thurnher M.** CD56+ human blood dendritic cells effectively promote TH1-type gammadelta T-cell responses. *Blood .* 2009, 114(20):4422-31.

66. **Silva-Santos B, Schamel WW, Fisch P, Eberl M.** γδ T-cell conference 2012: close encounters for the fifth time. *Eur J Immunol.* 2012, 42(12):3101-5.

67. **Roelofs AJ, Jauhiainen M, Mönkkönen H, Rogers MJ, Mönkkönen J, Thompson K.** Peripheral blood monocytes are responsible for gammadeltag T cell activation induced by zoledronic acid through accumulation of IPP/DMAPP. *Br J Haematol.* 2009, 144(2):245-50.

68. **Meuter S, Eberl M, Moser B.** Prolonged antigen survival and cytosolic export in cross-presenting human gammadelta T cells. *Proc Natl Acad Sci U S A.* 2010, 107(19):8730-5.

69. **Yao L, Zhang Y, Chen K, Hu X, Xu LX.** Discovery of IL-18 as a novel secreted protein contributing to doxorubicin resistance by comparative secretome analysis of MCF-7 and MCF-7/Dox. *PLoS One.* 2011, 6(9):e24684.

70. **Lanzavecchia A, Sallusto F.** Understanding the generation and function of memory T cell subsets. *Curr Opin Immunol.* 2005, 17(3):326-32.

71. **Hou L, Jie Z, Desai M, Liang Y, Soong L, Wang T, Sun J.** Early IL-17 production by intrahepatic T cells is important for adaptive immune responses in viral hepatitis. *J Immunol.* 2013, 190(2):621-9.

72. **Lalor SJ, Dungan LS, Sutton CE, Basdeo SA, Fletcher JM, Mills KH.** Caspase-1-processed cytokines IL-1beta and IL-18 promote IL-17 production by gammadelta and CD4 T cells that mediate autoimmunity. *J Immunol.* 2011, 186(10):5738-48.

9. List of Abbreviations

A. dest	aqua dest, lat. *aqua destillata*
APC	allophycocyanin
APCs	antigen presenting cells
APPI	1-adenosin-5′-yl ester 3-(3-methylbut-3-enyl) ester (novel ATP analogue)
ATP	adenosintriphosphat
BD	Becton Dickinson
BFA	Brefeldin A
Cat. No.	catalog number
CBA	Cytometric Bead Array
CCL2	chemokine (C-C motif) ligand 2
CD	cluster of differentiation
CDR3	complementarity-determining region 3
Cy7	cyanin 7
DC	dendritic cell
DETC	dendritic epidermal T cells
DMAPP	dimethylallyl pyrophosphate
DMSO	dimethylsulfoxid
EDTA	ethylenediaminetetraacetic Acid
ELISA	enzyme-linked immunosorbent assay
FACS	Fluorescence Activated Cell Sorting
FBS	fetal bovine serum
Fig	figure
FITC	fluoresceinisothiocyanat
FPP	farnesyl pyrophosphate
GGPP	geranylgeranyl pyrophosphate GlutaMAX L-glutamine
GM-CSF	granulocyte macrophage colony-stimulating factor
GTP	guanosine triphosphate
HBBS	Hank's Balanced Salt Solution

HMB-PP	(E)-4-hydroxy-3-methyl-but-2-enyl pyrophosphate
HMG-CoA	hydroxymethyl-glutaryl coenzyme A
ICAM-1	intercellular adhesion molecule 1
IEL	intraepithelial lymphocytes
IFN	interferon
IgG	immunoglobulin G
IL	interleukin
IL-2Rα	IL-2 receptor α chain
IPP	isopentenyl pyrophosphate
LD	Depletion Column
LS	Isolation Column
LSM	lymphocyte separation medium
MACS®	Magnetic Activated Cell Sorting
MBL	Medical & Biological Laboratories Co.
MHC	major histocompatibility complex
MICA	MHC class I chain-related molecules A
MICB	MHC class I chain-related molecules B
min	minutes
n.s	not significant
Na-Pyruvate	Sodium pyruvate
N-BP	nitrogen-containing bisphosphonate
NEAA	nonessential amino acids
NK cells	natural killer cells
NKG2D	natural killer group 2, member D
Order No.	order number
PBMCs	peripheral blood mononuclear cells
PBS	phosphat-bufferes saline
PE	phycoerythrin
PerCP-Cy5.5	peridinin chlorophyll protein cyanine 5.5
RAG	recombination activation gene
rhu IL	recombinant human interleukin
RPM	revolutions per minute
RPMI	Roswell Park Memorial Institute

RT	room temperature
SD	standard deviation
T_{CM}	central memory T cells
TCR	T cell receptor
T_{EM}	effector-memory T cells
T_{EMRA}	terminally differentiated T cells
Th cells	T helper cells
T_{naive}	naive T cells
TNF	tumour necrosis factor
ULBP	UL16-binding protein
YVAD	Ac-Tyr-Val-Ala-Asp-2,6-dimethylbenzoyloxymethyl-ketone (caspase I inhibitor V; IL-1β converting enzyme)
Zol	zoledronate

10. Curriculum vitae

10.1 Personal details

name and surname:	Juliana Komuczki
place of birth:	Innsbruck
birth date:	29.01.1990
nationality:	Austria

10.2 Work experience and Education

Scientific research

Nov 2012 – July 2013	**Master's internship (Junior Scientist) at Laboratory of Immunology and Immuntherapy, Department for Urology, Medical University of Innsbruck, Oncotyrol – K1 Center for Personalized Cancer Medicine** Master thesis: *"Mechanisms of zoledronate – induced immune activation"* Univ.-Prof. Dr. Martin Thurnher
July – Sep. 2012	**Research Associate at Baxter BioScience-Section of „Global Pathogen Safety & Virus Vaccines"** of Senior Director Thomas R. Kreil, Ph.D. *about Vaccine safety of Ross River Fever Virus* based on Good Laboratory Practice (GLP) Guidance and Good Documentation Practice (GDP) Guidance, biosafety level 3

May – July 2012	**Internship at Max F. Perutz Laboratories (MFPL) – Section of „Molecular Cell Biology“** in the working group of Dr. Kraft (Regulation and signaling in autophagy) about *“Seamless gene tagging (N- or C-terminal)”*
Mar. –May. 2012	**Internship at “St. Anna Kinderkrebsforschung” Children Cancer Research Institute (CCRI)** –**Molecular Biology of Solid Tumours** in the research laboratory of Prof. Kovar, *“SIRT1 in Ewing Sarcoma cell lines”*
July – Sep. 2011	**Scientifically pre-investment study at Biocenter Innsbruck Medical University –Section of Genomics and RNomics** in the research laboratory of Prof. Polacek, “*The E-Site Project – chemically engineered 23S rRNA for studies on protein biosynthesis“*
Aug. – Sep. 2010	**Internship at Department of Hygiene, Microbiology and Social medicine – Section of Hygiene and Medical Microbiology,** Univ.-Prof. C. Lass-Flörl
July – Aug. 2010	**Practical training at the University of Innsbruck-University at the research Laboratory of Molecular Immunology and Infectiology** and in routine Laboratory of Infection- and Immunodiagnostic, Univ.-Prof. Günter Weiss

Education	
Oct. 2011 – July 2013	MSc. In Molecular Biology (Molecular Medicine) at the University of Vienna **Master thesis:** *"Mechanisms of zoledronate – induced immune activation"* Univ.-Prof. Martin Thurnher
Sep. 2008 – July 2011	BSc. In Biology at the University of Innsbruck **Bachelor thesis:** *"Proto-Onkogene am Beispiel von RAS Proto-Onkogen"* Univ.-Prof. Bernhard Auer
Sep. 2000 - June 2008	High School diploma/"Matura" at Realgymnasium Reithmann (with scientific focus)

10.3 Scientific achievement

Oliver Nussbaumer, Georg Gruenbacher, Hubert Gander, Juliana Komuczki, Andrea Rahm, and Martin Thurnher. Essential Requirements of Zoledronate-Induced Cytokine and γδ T Cell Proliferative Responses. J Immunol 1300603; published ahead of print June 21, 2013, doi:10.4049/jimmunol.1300603

11. Lebenslauf

11.1 Persönliche Details

Vor- und Nachname	Juliana Komuczki
Geburtsort:	Innsbruck
Geburtstag:	29.01.1990
Staatsangehörigkeit:	Österreich

11.2 Berufliche Erfahrungen und Ausbildung

Facheinschlägige Berufspraktika

Juli – Aug. 2010	**Praktikum an der Innsbrucker-Universitätsklinik für Innere Medizin I im Forschungslabor für Molekulare Immunologie und Infektiologie bzw. im Routinelabor für Infektions-und Immundiagnostik** Univ.-Prof. Günter Weiss
Aug. – Sep. 2010	**Praktikum im Department für Hygiene, Mikrobiologie und Sozialmedizin - Sektion für Hygiene und Medizinische Mikrobiologie** Univ.-Prof. C. Lass-Flörl
Juli – Sep. 2011	**Forschungsnahe Projektstudie im Biocenter Innsbruck Medical University –Sektion für Genomik und RNomik**, Prof. Polacek, „*The E-Site Project – chemically engineered 23S rRNA for studies on protein biosynthesis“*

März –Mai. 2012	**Facheinschlägiges Praktikum in der St. Anna Kinderkrebsforschung** – über**„Molecular Biology of Solid Tumours“**, Prof. Kovar, *„SIRT1 in Ewing Sarcoma cell lines”*
Mai – Juli 2012	**Facheinschlägiges Praktikum in Max F. Perutz Laboratories – Sektion „Molecular Cell Biology“- „Regulation and signalling in autophagy“**, Dr. Kraft, *„Seamless gene tagging (N- or C-terminal)”*
Juli – Sep. 2012	**Wissenschaftlicher Mitarbeiter bei Baxter BioScience -Abteilung „Global Pathogen Safety & Virus Vaccines“**, Senior Director Thomas R. Kreil, Ph.D. *über Impfstoffentwicklung des „Ross River Fever Virus“* basierend auf „Good Laboratory Practice” (GLP) und „Good Documentation Practice” (GDP), biologische Sicherheits-stufe 3 (BSL-3)
Nov. 2012 – Juli 2013	**Masterarbeit (Nachwuchswissenschaftler) im Labor für Immunologie & Immuntherapie**, **Klinik für Urologie, Medizinische Universität Innsbruck, Oncotyrol - K1 Zentrum für personalisierte Krebsmedizin**, Univ.-Prof. Martin Thurnher; Masterarbeit**: “***Mechanisms of zoledronate-induced immune activation“*

Ausbildung	
Sep. 2000 - Juni 2008	Matura am Realgymnasium Reithmann in Innsbruck (mit naturwissenschaftlichen Schwerpunkt)
Sep. 2008 – Juli 2011	BSc. In Biologie an der Universität Innsbruck **Bachelorarbeit:** "*Proto-Onkogene am Beispiel von RAS Proto-Onkogen"* Univ.-Prof. Bernhard Auer
Oct. 2011 – Juli 2013	MSc. In Molekulare Biologie (Molekulare Medizin) an der Universität Wien **Masterarbeit:** *"Mechanisms of zoledronate – induced immune activation"* Univ.-Prof. Martin Thurnher

11.3 Wissenschaftliche Leistungen

Oliver Nussbaumer, Georg Gruenbacher, Hubert Gander, Juliana Komuczki, Andrea Rahm, and Martin Thurnher. Essential Requirements of Zoledronate-Induced Cytokine and γδ T Cell Proliferative Responses. J Immunol 1300603; published ahead of print June 21, 2013, doi:10.4049/jimmunol.1300603